


Accelerating Reductions Using Graph Neural Networks and a New Concurrent Local Search for the Maximum Weight Independent Set Problem

Ernestine Großmann ✉ 

Heidelberg University, Faculty of Mathematics and Computer Science, Germany

Kenneth Langedal¹ ✉ 

University of Bergen, Department of Informatics, Norway

Christian Schulz ✉ 

Heidelberg University, Faculty of Mathematics and Computer Science, Germany

Abstract

The MAXIMUM WEIGHT INDEPENDENT SET problem is a fundamental NP-hard problem in combinatorial optimization with several real-world applications. Given an undirected vertex-weighted graph, the problem is to find a subset of the vertices with the highest possible weight under the constraint that no two vertices in the set can share an edge. An important part of solving this problem in both theory and practice is data reduction rules, which several state-of-the-art algorithms rely on. However, the most complicated rules are often not used in applications since the time needed to check them exhaustively becomes infeasible. In this work, we introduce three main results. First, we introduce several new data reduction rules and evaluate their effectiveness on real-world data. Second, we use a machine learning screening algorithm to speed up the reduction phase, thereby enabling more complicated rules to be applied. Our screening algorithm consults a Graph Neural Network oracle to decide if the probability of successfully reducing the graph is sufficiently large. For this task, we provide a dataset of labeled vertices for use in supervised learning. We also present the first results for this dataset using established Graph Neural Network architectures. Third, we present a new concurrent metaheuristic called CONCURRENT DIFFERENCE-CORE HEURISTIC. On the reduced instances, we use our new metaheuristic combined with iterated local search, called CHILS (CONCURRENT HYBRID ITERATED LOCAL SEARCH). For this iterated local search, we provide a new implementation specifically designed to handle large graphs of varying densities. CHILS outperforms the current state-of-the-art on all commonly used benchmark instances, especially the largest ones.

2012 ACM Subject Classification Theory of computation → Design and analysis of algorithms

Keywords and phrases randomized local search, graph neural networks, data reductions, maximum weight independent set, algorithm engineering

Funding

Ernestine Großmann: Supported by DFG grant SCHU 2567/3-1.

Kenneth Langedal: Supported by the Research Council of Norway under contract 303404 and Meltzer Research Fund, project number 104066111.

Acknowledgements The inspiration for this work and collaboration started at the Dagstuhl Seminar 23491 on Scalable Graph Mining and Learning [41]. We also thank Fredrik Manne for his helpful feedback throughout the writing process.

¹ Corresponding author

1 Introduction

Consider an undirected vertex-weighted graph $G = (V, E, \omega)$, where V is the set of vertices, E is the set of edges, and $\omega : V \rightarrow \mathbb{R}^+$ is a function that maps each vertex to a positive weight. An *independent set* $\mathcal{I} \subseteq V$ is a subset of the vertices such that no two members of the independent set share an edge, i.e. for all $u, v \in \mathcal{I}$ it holds that $\{u, v\} \notin E$. The MAXIMUM WEIGHT INDEPENDENT SET (MWIS) problem asks for an independent set \mathcal{I} of maximum weight, where the weight of \mathcal{I} is defined as the sum $\sum_{v \in \mathcal{I}} \omega(v)$ of the vertices. MWIS is a generalization of the classical NP-hard problem MAXIMUM INDEPENDENT SET (MIS), where all weights equal one. For MIS and MWIS, the complement of a solution forms a minimum (weighted) vertex cover. A *vertex cover* $C \subseteq V$ is a set of vertices that cover all the edges, i.e. for all $\{u, v\} \in E$ we have $u \in C$ or $v \in C$. For all practical purposes, the problem of finding a maximum independent set is equivalent to that of finding a minimum vertex cover. The decision version of the MINIMUM VERTEX COVER (MVC) problem was one of Karp’s original 21 NP-complete problems [37].

The MWIS problem and other closely related problems have several practical applications ranging from matching molecular structures to wireless networks [12]. Recently, Dong et al. [19] introduced a new collection of instances based on real-life long-haul vehicle routing problems at Amazon. The problem they want to solve is to find a subset of vehicle routes such that no two routes share a driver or a load. Each route has a weight, and the objective is to maximize the sum of the route weights. To state this problem as a MWIS, they build a conflict graph where vertices correspond to routes and the route weights are modeled by vertex weights. Furthermore, they connect two vertices by an edge if the corresponding routes have a conflict, i.e. they share a driver or a load. For a further, more detailed overview of applications, see Butenko [12].

It is well known that data reduction rules can speed up algorithms for NP-hard problems. They reduce an instance in such a way that an optimal solution for the reduced instance can be lifted to an optimal solution for the original instance. Several reduction rules have been developed for MIS and MWIS. Additionally, reduction rules have also improved many heuristic approaches for MWIS and associated problems. Such reduction rules are often used as a preprocessing step before running an exact algorithm or heuristic on the reduced graph.

Our Results

Our contribution is two-fold: first, we developed an advanced, exact preprocessing tool called LEARNANDREDUCE that employs Graph Neural Networks (GNNs) to decide where to apply data reduction rules. In addition to existing rules (see [24, 29, 44, 64, 65]), we propose new data reduction rules that can reduce the instances even further. With our GNN filtering, we can now apply reduction rules that were previously unused in other works due to the computational cost required to determine their applicability [28]. Second, we propose a new concurrent iterated local search heuristic CHILS to compute large-weight independent sets very fast. In particular, our heuristic works by alternating between the full graph and the DIFFERENCE-CORE (D-CORE) which is a subgraph constructed using multiple heuristic solutions. With this heuristic and LEARNANDREDUCE we are able to outperform existing heuristics across a wide variety of real-world instances. Our main results can be summarized as follows.

- We introduce seven new data reduction rules for the MWIS problem.
- We present a new dataset with labeled vertices for the problem of early reduction rule screening. The dataset contains two collections of graphs, one with unreduced instances

and one after running a set of fast reductions. The second is the one we use for the early reduction rule screening, and it consists of more than one million labeled vertices.

- Using LEARNANDREDUCE, we can reduce our instances to within one percent of what is possible using the full set of reduction rules while spending less than 23% of the corresponding time. These results are adjusted for fast reduction rules that would always be applied.
- For a large set of real-world test instances accumulated over several years by earlier works, CHILS combined with LEARNANDREDUCE finds the best solution across *all* test instances. This result is kept separate from the new vehicle routing instances [19] due to the significant differences in size and difficulty.
- On vehicle routing instances, we compare CHILS with two recent heuristics, METAMIS [18] and a recent Bregman-Sinkhorn algorithm [30], both designed specifically for these instances. Even though CHILS is not optimized for vehicle routing instances and, in contrast to the competitors, does not make use of the additional clique information provided for these instances, it still finds the best solution on 31/37 instances while being significantly closer to the best competitor in the cases where CHILS is not best.
- Running CHILS in parallel significantly improves performance to the point where CHILS computes the best solution on 35/37 instances. These results are with one-hour time limit and the same 16-core CPU used to evaluate all the heuristics. For parallel scalability, we include experiments on a 128-core CPU where the parallel version of CHILS reaches speedups of up to 104 compared to the sequential version.

2 Preliminaries

In this work, a graph $G = (V, E, \omega)$ is an undirected vertex-weighted graph with $n = |V|$ and $m = |E|$, where $V = \{0, \dots, n-1\}$ and $\omega : V \rightarrow \mathbb{R}^+$. The neighborhood $N(v)$ of a vertex $v \in V$ is defined as $N(v) = \{u \in V \mid \{u, v\} \in E\}$. Additionally, we define $N[v] = N(v) \cup \{v\}$. The same sets are defined for the neighborhood $N(U)$ of a set of vertices $U \subset V$, i.e. $N(U) = \cup_{v \in U} N(v) \setminus U$ and $N[U] = N(U) \cup U$. The degree $\deg(v)$ of a vertex is defined as the number of its neighbors $\deg(v) = |N(v)|$. The complement graph is defined as $\bar{G} = (V, \bar{E})$, where $\bar{E} = \{\{u, v\} \mid \{u, v\} \notin E\}$ is the set of edges not present in G . Furthermore, for a graph $G = (V, E)$ we define an induced subgraph $G[S]$ on a subset of vertices $S \subset V$ by $G[S] = (S, \{\{u, v\} \in E \mid u, v \in S\})$. For $S \subset V$, we use the notation $G - S$ instead of $G[V \setminus S]$. Similarly for a single vertex $v \in V$, we abbreviate $G[V \setminus \{v\}]$ to $G - v$. A set $I \subseteq V$ is called an *independent set* (IS) if for all vertices $u, v \in I$ there is no edge $\{u, v\} \in E$. For a given IS \mathcal{I} , a vertex $v \notin \mathcal{I}$ is called free if $\mathcal{I} \cup \{v\}$ is still an independent set. An IS is called *maximal* if there are no free vertices. The MAXIMUM INDEPENDENT SET problem (MIS) is that of finding an IS with maximum cardinality. Similarly, the MAXIMUM WEIGHT INDEPENDENT SET problem (MWIS) is that of finding an IS with maximum weight. The weight of an independent set \mathcal{I} is defined as $\omega(\mathcal{I}) = \sum_{v \in \mathcal{I}} \omega(v)$ and $\alpha_\omega(G)$ denotes the weight of an MWIS of G . The complement of a maximal independent set is a *vertex cover*, i.e. a subset $C \subseteq V$ such that every edge $e \in E$ is covered by at least one vertex $v \in C$. An edge is *covered* if it is incident to one vertex in the set C . The MINIMUM VERTEX COVER problem, defined as computing a vertex cover with minimum cardinality, is thereby dual to the MIS problem. Another closely related concept is cliques. A *clique* is a set $Q \subseteq V$ such that all vertices are pairwise adjacent. A clique in the complement graph \bar{G} corresponds to an independent set in the original graph G . A vertex is called *simplicial* when its neighborhood forms a clique.

3 Related Work

We give an overview of latest work on both exact and heuristic procedures for MWIS. For a full overview of the related work on MWIS, MWVC, and MAXIMUM WEIGHTED CLIQUE solvers, as well as all known reduction rules for the MWIS and MWVC problems, we defer to the recent survey [28]. For more general details on data reduction techniques, we refer the reader to the survey [4].

3.1 Exact Methods

Exact algorithms usually compute optimal solutions by systematically exploring the solution space. *Branch-and-bound* is a frequently used paradigm in exact algorithms for combinatorial optimization problems [53, 60]. In the case of MWIS, branch-and-bound algorithms compute optimal solutions by case distinctions where vertices are either included in the current solution or excluded from it, branching into two subproblems. Over the years, branch-and-bound methods have been improved by new branching schemes or better pruning methods using upper and lower bounds to exclude specific subtrees [8, 9, 49]. In particular, Warren and Hicks [60] proposed three branch-and-bound algorithms that combine the use of weighted clique covers and a branching scheme first introduced by Balas and Yu [9]. Their first approach extends the algorithm by Babel [8] by using more intricate data structures to improve performance. The second one is an adaptation of the algorithm of Balas and Yu, which uses a weighted clique heuristic that yields structurally similar results to the algorithm of Balas and Yu. The last algorithm is a hybrid version that combines both algorithms and can compute optimal solutions on graphs with hundreds of vertices.

In recent years, reduction rules have frequently been added to branch-and-bound methods yielding so-called *branch-and-reduce* algorithms [5]. Branch-and-reduce algorithms often outperform branch-and-bound algorithms by applying reduction rules between each branching step. For the unweighted case, many branch-and-reduce algorithms have been developed in the past. The currently best exact solver [35], which won the PACE challenge 2019 [35, 57], uses a portfolio of branch-and-reduce/bound solvers for the complementary problems. For non-portfolio solvers, Plachetta et al. [54] improved on the branch-and-reduce approach by using SAT solvers for additional pruning. Recently, novel branching strategies have been presented by Hesse et al. [34] and later enhanced by Langedal et al. [45] to improve both branch-and-bound and branch-and-reduce approaches further.

The first branch-and-reduce algorithm for the weighted case was presented by Lamm et al. [44]. The authors first introduce two meta-reductions called neighborhood removal and neighborhood folding, from which they derive a new set of weighted reduction rules. On this foundation, a branch-and-reduce algorithm was developed using pruning with weighted clique covers similar to the approach by Warren and Hicks [60] for upper bounds and an adapted version of the ARW local search [7] for lower bounds. The exact algorithm by Lamm et al. was then extended by Gellner et al. [24] to utilize different variants of a transformation called *struction*, originally introduced by Ebenegger et al. [20] and later improved by Alexe et al. [6]. In contrast to previous reduction rules, *struction* transformations do not necessarily decrease the graph size but rather transform the graph, which later can lead to even further reduction. These variants were integrated into the framework of Lamm et al. in the preprocessing as well as in the reduction step. The experimental evaluation shows that this algorithm can solve a large set of real-world instances and outperforms the original branch-and-reduce algorithm by Lamm et al. as well as different state-of-the-art heuristic approaches such as the heuristic HILS by Nogueira [52] and two other local search algorithms DYNWVC1 and DYNWVC2

by Cai et al. [14]. Furthermore, a new branch-and-reduce algorithm was recently introduced using two new reduction rules [68].

Recently, Xiao et al. [64] also presented a branch-and-bound algorithm using reduction rules working especially well on sparse graphs. They undertake a detailed analysis of the running time bound on special graphs in their theoretical work. With the measure-and-conquer technique, they can show that the running time of their algorithm is $\mathcal{O}^*(1.1443^{(0.624x-0.872)n})$ where x is the average degree of the graph. This improves previous time bounds using polynomial space complexity for graphs of average degree up to three.

Figiel et al. [23] introduced a new idea to the state-of-the-art way of applying reductions. They propose not only to perform reductions but also the possibility of undoing them during the reduction process. They showed for the unweighted MVC problem that this can lead to new possibilities for applying further reductions and lead to smaller reduced graphs.

Finally, there are exact procedures that are either based on other extensions of the branch-and-bound paradigm [55, 61, 62], or on the reformulation into other NP-hard problems, for which a variety of solvers already exist. For instance, Xu et al. [67] developed an algorithm called SBMS that calculates an optimal solution for a given MWVC instance by solving a series of SAT instances. Also, for the MWVC problem, a new exact algorithm using the branch-and-bound idea combined with data reduction rules was recently presented [59]. We also note that several recent works on the complementary maximum weighted clique problem can handle large real-world networks [21, 33, 36]. However, using these solvers for the MWIS problem requires computing the complement graph. Since large real-world networks are often very sparse, processing their complements quickly becomes infeasible due to their memory requirement.

3.2 Heuristic Methods

Local search is a widely used heuristic approach for MWIS. This starts from any feasible solution and then tries to improve it by simple insertion, removal, or swap operations. Local search generally offers no theoretical guarantees for the solution quality. However, in practice, it often finds high-quality solutions significantly faster than exact procedures. For unweighted graphs, the iterated local search (ARW) by Andrade et al. [7] is a very successful heuristic. It is based on so-called (1,2)-swaps that removes one vertex from the solution and adds two new vertices, thus improving the current solution by one. Their heuristic uses special data structures that find such a (1,2)-swap in linear time in the number of edges or prove that none exists. Their heuristic is able to find (near-)optimal solutions for small to medium-size instances in milliseconds but struggles on large sparse instances with millions of vertices.

The hybrid iterated local search (HILS) by Nogueira et al. [52] adapts the ARW algorithm for weighted graphs. In addition to weighted (1,2)-swaps, it also uses $(\omega, 1)$ -swaps that adds one vertex v into the current solution and excludes its neighbors. These two types of neighborhoods are explored separately using variable neighborhood descent (VND). When it was introduced, their algorithm found optimal solutions on well-known benchmark instances within milliseconds and outperformed other state-of-the-art local search heuristics.

Two other local search heuristics, DYNWVC1 and DYNWVC2, for the complementary minimum weight vertex cover (MWVC) problem were presented by Cai et al. [14]. Their heuristic extend the existing FASTWVC heuristic [51] by dynamic selection strategies for vertices to be removed from the current solution. In practice, DYNWVC1 outperforms previous MWVC heuristics on map labeling instances and large-scale networks. DYNWVC2 provides further improvements on large-scale networks but performs worse on map labeling instances.

Li et al. [50] presented a local search heuristic NUMWVC for the MWVC problem.

Their heuristic applies reduction rules during the construction phase of the initial solution. Furthermore, they adapt the configuration checking approach [15] to the MWVC problem, which is used to reduce cycling, i.e. returning to a solution that has been visited recently. Finally, they develop a technique called self-adaptive vertex-removing, which dynamically adjusts the number of removed vertices per iteration. Experiments showed that NUMWVC outperformed state-of-the-art approaches on graphs of up to millions of vertices.

A hybrid method was recently introduced by Langedal et al. [46] to solve the MWVC problem. For this approach, they combined elements from exact methods with local search, data reductions, and graph neural networks. In their experiments, they achieve clear improvements compared to DYNWVC2, HILS, and NUMWVC in both solution quality and running time.

With EVOMIS, Lamm et al. [42] presented an evolutionary approach to tackle the maximum independent set problem. The key feature of their heuristic was to use graph partitioning to come up with natural combine operations, where whole blocks of solutions can be exchanged easily. Local search algorithms were added to these combine operations to improve the solutions further.

Combining the branch-and-reduce approach with the evolutionary algorithm EVOMIS, a reduction evolution algorithm REDUMIS was presented by Lamm et al. [43]. In their experiments, REDUMIS outperformed the local search ARW as well as the pure evolutionary approach EVOMIS. Another reduction-based heuristic HTWIS was presented recently by Gu et al. [29]. They repeatedly apply reductions exhaustively and then choose one vertex by a tie-breaking policy to add to the solution. Once this vertex and its neighbors has been removed from the graph, the reduction rules can be applied again. Their experiments show a significant improvement in running time. Recently, Großmann et al. [27] introduced a heuristic combining data reduction rules with an evolutionary approach. Here, the authors make use of exact data reductions and heuristic reductions derived from the population to reduce the graph iteratively. With this technique, they are able to achieve near-optimal solutions for a wide set of instances.

A new metaheuristic was introduced by Dong et al. [18], particularly for the vehicle routing instances introduced by Dong et al. [19]. With their metaheuristic METAMIS, they developed a local search heuristic using a new variant of path-relinking to escape local optima. In their experiments, they outperform the HILS heuristic on a wide range of instances, both in terms of time and solution quality. The vehicle routing instances come equipped with initial warm start solutions and clique information derived from the application. Using this clique information, Haller and Savchynskyy [30] proposed a Bregman-Sinkhorn algorithm that addresses a family of clique cover LP relaxations. In addition to solving the relaxed dual problem, they utilize a simple and efficient primal heuristic to obtain feasible integer solutions for the initial non-relaxed problem. In their experiments, they outperform METAMIS on time and solution quality, but only in the cold-start configuration where METAMIS does not use the precomputed solutions.

4 Learn and Reduce - GNN Guided Preprocessing

In this section, we introduce LEARNANDREDUCE, our new exact preprocessing technique that reduces the input graph efficiently using data reductions and Graph Neural Networks (GNNs).

In Section 4.1, we introduce several new data reduction rules for the MWIS problem. Some new reductions and existing ones need to solve additional MWIS problems on subgraphs, meaning preprocessing using these rules could take exponential time. For practical use, the

more costly reductions are limited in some way, especially for large instances. This is done, for example, by limiting the degree of the vertex to apply the reduction on, the subgraph size, or the time spent on each vertex. In Section 4.2, we introduce a new GNN application in the form of early data-reduction screening. We also provide a new and openly available supervised-learning dataset with graphs and labeled vertices for each reduction rule. At inference, for each expensive data reduction rule, a pre-trained GNN model decides what vertices should be checked for the applicability of the rule.

4.1 New Data Reduction Rules

This section introduces our new data reduction rules for the MWIS problem following the scheme used in [28]. For every reduction rule, we first describe the pattern that can be reduced by the corresponding rule. Afterwards, the information for the construction of the *reduced graph*, called G' is given. Then, the *offset* describes the difference between the weight of an MWIS on the reduced graph $\alpha_\omega(G')$ and the weight of an MWIS on the original graph $\alpha_\omega(G)$. Lastly, the information on how the solution on the reduced instance, called \mathcal{I}' , can be reconstructed to a solution on the original graph, called \mathcal{I} , is provided. In addition to including or excluding vertices directly, some reduction rules combine multiple vertices into potentially new vertices. We call this combine procedure *folding*. Including or excluding the folded vertices in \mathcal{I} only depends on whether the vertices they are folded into are included in \mathcal{I}' . Since our new reduction rules are extensions of or proven by other reduction rules, these are presented first.

Reduction 1.1 (Simplicial Vertex by Lamm et al. [44])

Let $v \in V$ be simplicial with maximum weight in its neighborhood, i.e. $\omega(v) \geq \max\{\omega(u) \mid u \in N(v)\}$, then include v .

$$\begin{array}{ll} \text{Reduced Graph} & G' = G - N[v] \\ \text{Offset} & \alpha_\omega(G) = \alpha_\omega(G') + \omega(v) \\ \text{Reconstruction} & \mathcal{I} = \mathcal{I}' \cup \{v\} \end{array}$$

Reduction 1.2 (Domination by Lamm et al. [44])

Let $u, v \in V$ be adjacent vertices such that $N[u] \subseteq N[v]$. If $\omega(v) \leq \omega(u)$, then exclude v .

$$\begin{array}{ll} \text{Reduced Graph} & G' = G - v \\ \text{Offset} & \alpha_\omega(G) = \alpha_\omega(G') \\ \text{Reconstruction} & \mathcal{I} = \mathcal{I}' \end{array}$$

Reduction 1.3 (Twin by Lamm et al. [44])

Let $u, v \in V$ have equal, independent neighborhoods $N(u) = N(v) = \{p, q, r\}$.

- If $\omega(\{u, v\}) \geq \omega(\{p, q, r\})$, then include u and v .

$$\begin{array}{ll} \text{Reduced Graph} & G' = G - N[\{u, v\}] \\ \text{Offset} & \alpha_\omega(G) = \alpha_\omega(G') + \omega(u) + \omega(v) \\ \text{Reconstruction} & \mathcal{I} = \mathcal{I}' \cup \{u, v\} \end{array}$$

- If $\omega(\{u, v\}) < \omega(\{p, q, r\})$ but $\omega(\{u, v\}) > \omega(\{p, q, r\}) - \min\{\omega(x) \mid x \in \{p, q, r\}\}$, then fold u, v, p, q, r into a new vertex v' .

<i>Reduced Graph</i>	$G' = G[(V \cup \{v'\}) \setminus (N[v] \cup \{u\})]$ with $N(v') = N(\{p, q, r\})$ and $\omega(v') = \omega(\{p, q, r\}) - \omega(\{u, v\})$.
<i>Offset</i>	$\alpha_\omega(G) = \alpha_\omega(G') + \omega(\{u, v\})$
<i>Reconstruction</i>	If $v' \in \mathcal{I}'$, then $\mathcal{I} = (\mathcal{I}' \setminus \{v'\}) \cup \{p, q, r\}$, else $\mathcal{I} = \mathcal{I}' \cup \{u, v\}$

Reduction 1.4 (Heavy Set by Xiao et al. [65])

Let u and v be non-adjacent vertices having at least one common neighbor x . If for every independent set $\tilde{\mathcal{I}}$ in the induced subgraph $G[N(\{u, v\})]$, $\omega(N(\tilde{\mathcal{I}}) \cap \{u, v\}) \geq \omega(\tilde{\mathcal{I}})$, then include u and v .

<i>Reduced Graph</i>	$G' = G - N[\{u, v\}]$
<i>Offset</i>	$\alpha_\omega(G) = \alpha_\omega(G') + \omega(u) + \omega(v)$
<i>Reconstruction</i>	$\mathcal{I} = \mathcal{I}' \cup \{u, v\}$

Domination Based Reductions

We derive the following two reduction rules by extending Reduction 1.2 first introduced by Lamm et al. [44]. The idea of the original domination rule is to find two adjacent vertices $u, v \in V$ where any independent set including v can be transformed into an equal or higher weight independent set by replacing v with u .

In the extended domination rule, see Reduction 1.5, instead of removing vertices, we remove edges and reduce vertex weights. With this reduction rule, we allow two adjacent vertices u and v to be both in the solution on the reduced instance. If the edge removal leads to a solution including both vertices, we remove the previously dominated, lower weight vertex from the solution in the restoring process. With this reduction rule, we sparsify the graph and potentially make other rules applicable.

Reduction 1.5 (Extended Domination)

Let $u, v \in V$ be adjacent vertices such that $N[u] \subseteq N[v]$. If $\omega(v) > \omega(u)$, then we remove the edge between u and v .

<i>Reduced Graph</i>	$G' = (V, E \setminus \{u, v\})$ and $\omega(v) = \omega(v) - \omega(u)$
<i>Offset</i>	$\alpha_\omega(G) = \alpha_\omega(G')$
<i>Reconstruction</i>	If $v \in \mathcal{I}'$, then $\mathcal{I} = \mathcal{I}' \setminus \{u\}$, else $\mathcal{I} = \mathcal{I}'$

Proof. Let $u, v \in V$ be adjacent vertices such that $N[u] \subseteq N[v]$ and $\omega(v) > \omega(u)$. Further, let G' be the reduced graph after applying the reduction to u and v . We use u' and v' to refer to u and v in G' . First, we consider the case that $v' \in \mathcal{I}'$ and show that $\mathcal{I} = \mathcal{I}' \setminus \{u'\}$ is an MWIS in G . Since $N[u] \subseteq N[v]$ and $v' \in \mathcal{I}'$ it holds that $u' \in \mathcal{I}'$, because \mathcal{I}' is maximal. Now, assume there is an MWIS $\tilde{\mathcal{I}}$ in G with $\omega(\tilde{\mathcal{I}}) > \omega(\mathcal{I})$. Then, the MWIS $\tilde{\mathcal{I}}$ is also an independent set in the reduced instance and $\omega(\tilde{\mathcal{I}}) > \omega(\mathcal{I}' \setminus \{u'\}) + \omega(u) = \omega(\mathcal{I}' \setminus \{u', v'\}) + \omega(v) - \omega(u) + \omega(u) = \omega(\mathcal{I}' \setminus \{u', v'\}) + \omega(v') + \omega(u') = \omega(\mathcal{I}')$. This contradicts that \mathcal{I}' is an MWIS in G' . Furthermore, since \mathcal{I}' is an independent set and we only removed u to obtain \mathcal{I} , the independent set property still holds and therefore \mathcal{I} is an MWIS in G .

We prove the second case $v' \notin \mathcal{I}'$ in the same way. Here, \mathcal{I}' is also an independent set in G . Since $v' \notin \mathcal{I}'$ it holds that the weight of \mathcal{I}' is the same in G and G' . Therefore, there can not exist an independent set of higher weight than \mathcal{I}' in G , since this would also exist in the reduced instance contradicting \mathcal{I}' being an MWIS in G' . ◀

Additionally, we add a reduction rule which reverses Reduction 1.5. This way, we can add back edges that were previously removed and introduce new edges later in the reduction process.

Reduction 1.6 (Extended Domination Reversed)

Let $u, v \in V$ be non-adjacent vertices such that $N(u) \subseteq N(v)$. If $\omega(u) + \omega(v) < \omega(N(v))$, then we can add an edge between u and v .

Reduced Graph	$G' = (V, E \cup \{u, v\})$ and $\omega(v) = \omega(v) + \omega(u)$
Offset	$\alpha_\omega(G) = \alpha_\omega(G')$
Reconstruction	If $v \in \mathcal{I}'$, then $\mathcal{I} = \mathcal{I}' \cup \{u\}$, else $\mathcal{I} = \mathcal{I}'$

Proof. Let $u, v \in V$ be non-adjacent vertices such that $N(u) \subseteq N(v)$ and $\omega(u) + \omega(v) < \omega(N(v))$. Further, let G' be the reduced graph after applying the reduction to u and v . We use u' and v' to refer to u and v in G' . Note that since $\omega(v') = \omega(v) + \omega(u)$ the weight $\omega(\mathcal{I}) = \omega(\mathcal{I}')$. First, we consider the case that $v' \in \mathcal{I}'$. We show that $\mathcal{I} = \mathcal{I}' \cup \{u'\}$ is an MWIS in G . Since $v' \in \mathcal{I}'$ and u' and v' are adjacent in G' it holds that $u' \notin \mathcal{I}'$. Now, assume there is a MWIS $\tilde{\mathcal{I}}$ in G with $\omega(\tilde{\mathcal{I}}) > \omega(\mathcal{I})$. We only consider the case where $u, v \in \tilde{\mathcal{I}}$, since otherwise, either $\tilde{\mathcal{I}}$ is not maximal, or $\mathcal{I}, \mathcal{I}'$ and $\tilde{\mathcal{I}}$ are all equal. With $u, v \in \tilde{\mathcal{I}}$ we construct an independent set $\tilde{\mathcal{I}}' = \tilde{\mathcal{I}} \setminus \{u, v\} \cup \{v'\}$ in G' . It holds that $\omega(\tilde{\mathcal{I}}') = \omega(\tilde{\mathcal{I}})$ since $\omega(v') = \omega(v) + \omega(u)$. Since \mathcal{I}' is an MWIS in G' , it follows that $\omega(\mathcal{I}') \geq \omega(\tilde{\mathcal{I}}')$. Now, $\omega(\mathcal{I}) < \omega(\tilde{\mathcal{I}}) = \omega(\tilde{\mathcal{I}}') \leq \omega(\mathcal{I}')$ which contradicts that $\omega(\mathcal{I}) = \omega(\mathcal{I}')$. For the case of $v \notin \mathcal{I}'$ it holds that the weights and sets are directly equivalent between G and G' , and therefore $\mathcal{I} = \mathcal{I}'$ is an MWIS in G . \blacktriangleleft

► **Remark 1.** Initially, the concept of adding edges as described in Reduction 1.6 may seem counter-intuitive since the goal is to reduce the graph size. However, this approach is particularly valuable for more complex reduction rules that involve solving independent sets within neighborhoods. By adding edges, additional vertices are incorporated into the direct neighborhood. This expansion can potentially enable further applications of other reduction rules, such as Reduction 1.4 or 1.10.

Twin Based Reductions

Reduction 1.3 can be generalized to also be applied if the neighborhood is larger than three vertices or when it is not an independent set. The main idea is that for any two vertices that have an equal neighborhood any maximal solution always includes either both or none of these vertices. Therefore, we can fold the two twin vertices. In some special cases we can also fold these twin vertices with their neighborhood.

Reduction 1.7 (Extended Twin)

Let $u, v \in V$ be non-adjacent and with equal neighborhoods $N(u) = N(v)$. Let further $\mathcal{I}_{N(v)}$ be an MWIS on $G[N(v)]$.

- If $\omega(u) + \omega(v) \geq \omega(\mathcal{I}_{N(v)})$, then include u and v .

Reduced Graph	$G' = G - N[\{u, v\}]$
Offset	$\alpha_\omega(G) = \alpha_\omega(G') + \omega(u) + \omega(v)$
Reconstruction	$\mathcal{I} = \mathcal{I}' \cup \{u, v\}$

- If $\omega(u) + \omega(v) < \omega(\mathcal{I}_{N(v)})$ but $\mathcal{I}_{N(v)}$ is the only independent set in $N(v)$ with this property, then fold u, v , and $N(v)$ into v' .

$$\begin{array}{ll}
\text{Reduced Graph} & G' = G[(V \cup \{v'\}) \setminus N[\{u, v\}]] \text{ with } N(v') = N(N[\{u, v\}]) \\
& \text{and } \omega(v') = \omega(\mathcal{I}_{N(v)}) - \omega(u) - \omega(v) \\
\text{Offset} & \alpha_\omega(G) = \alpha_\omega(G') + \omega(u) + \omega(v) \\
\text{Reconstruction} & \text{If } v' \in \mathcal{I}', \text{ then } \mathcal{I} = (\mathcal{I}' \setminus \{v'\}) \cup \mathcal{I}_{N(v)}, \text{ else } \mathcal{I} = \mathcal{I}' \cup \{u, v\}
\end{array}$$

■ Otherwise, fold u and v into a new vertex v' .

$$\begin{array}{ll}
\text{Reduced Graph} & G' = G[(V \cup \{v'\}) \setminus \{u, v\}] \text{ with } N(v') = N(\{u, v\}) \text{ and } \omega(v') = \omega(v) + \omega(u) \\
\text{Offset} & \alpha_\omega(G) = \alpha_\omega(G') \\
\text{Reconstruction} & \text{If } v' \in \mathcal{I}', \text{ then } \mathcal{I} = \mathcal{I}' \setminus \{v'\} \cup \{u, v\}, \text{ else } \mathcal{I} = \mathcal{I}'
\end{array}$$

Proof. Let $u, v \in V$ be twin vertices, i.e. non-adjacent vertices such that $N(u) = N(v)$. Since they share the same neighborhood, there is no maximal solution that only includes one of these vertices. Therefore, we can fold the two vertices into a new vertex v' with weight $\omega(v') = \omega(v) + \omega(u)$ as is done in the third case. For the first case, if $\omega(u) + \omega(v) \geq \omega(\mathcal{I}_{N(v)})$ and there is a solution \mathcal{I} not including v' , then we can always construct an equal or better solution $\mathcal{I}' = \mathcal{I} \setminus N(v) \cup \{u, v\}$ and therefore we can include the vertices u and v .

In the second case, we first assume that $v' \in \mathcal{I}$ and show that $\omega(\mathcal{I}_{N(v)}) + \alpha_\omega(G - N[N[v]]) \geq \omega(v) + \omega(u) + \alpha_\omega(G - N[v])$. This implies that the set $\mathcal{I}_{N(v)}$ is contained in some MWIS of G . Since $v' \in \mathcal{I}$ we know that

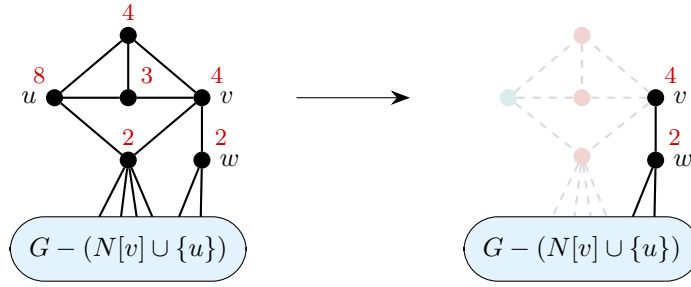
$$\begin{aligned}
\omega(u) + \omega(v) + \alpha_\omega(G') &= \omega(u) + \omega(v) + \omega(v') + \alpha_\omega(G' - N_{G'}[v']) \\
&= \omega(u) + \omega(v) + \omega(\mathcal{I}_{N(v)}) - \omega(u) - \omega(v) + \alpha_\omega(G' - N_{G'}[v']) \\
&= \omega(\mathcal{I}_{N(v)}) + \alpha_\omega(G' - N_{G'}[v']).
\end{aligned}$$

Since \mathcal{I}' is an MWIS of G' , we have $\omega(u) + \omega(v) + \alpha_\omega(G') \geq \omega(u) + \omega(v) + \alpha_\omega(G' - v') = \omega(u) + \omega(v) + \alpha_\omega(G - N[v])$. Now suppose that $v' \notin \mathcal{I}$. For this case we show $\omega(u) + \omega(v) + \alpha_\omega(G - N[v]) \geq \omega(\mathcal{I}_{N(v)}) + \alpha_\omega(G - N[N[v]])$, which implies that u and v are in some MWIS of G . Since now $v \notin \mathcal{I}'$, we get $\omega(u) + \omega(v) + \alpha_\omega(G') = \omega(u) + \omega(v) + \alpha_\omega(G' - v') = \omega(u) + \omega(v) + \alpha_\omega(G - N[v])$. As \mathcal{I}' is an MWIS of G' , we also get

$$\begin{aligned}
\omega(u) + \omega(v) + \alpha_\omega(G') &\geq \omega(u) + \omega(v) + \omega(v') + \alpha_\omega(G' - N_{G'}[v']) \\
&= \omega(u) + \omega(v) + \omega(\mathcal{I}_{N(v)}) - \omega(u) - \omega(v) + \alpha_\omega(G - N[N[v]]) \\
&= \omega(\mathcal{I}_{N(v)}) + \alpha_\omega(G - N[N[v]]).
\end{aligned}$$

Since $\mathcal{I}_{N(v)}$ is the only independent set in $G(N[v])$ with higher weight than $\omega(u) + \omega(v)$ v is in some MWIS of G . We get $\alpha_\omega(G) = \omega(u) + \omega(v) + \alpha_\omega(G - N[v]) = \omega(u) + \omega(v) + \alpha_\omega(G')$. ◀

Note that the third case of Reduction 1.7 is already used in [1] but not introduced in this way by Lamm et al. [44]. Now we extend the idea of Reduction 1.7. For the following reduction rule we no longer require the neighborhoods of the two vertices u and v to be equal, but assume that $N(u) \subseteq N(v)$. If $\omega(u) + \omega(v) \geq \omega(N(v))$ the vertex u is always in an MWIS. The idea is that we can always replace vertices $x \in N(v)$ in a solution with u and v and thereby get an equal or better solution.



■ **Figure 1** Illustration of the Almost Twin (Reduction 1.8). In the original graph on the left, $N(u) \subseteq N(v)$ with $\omega(u) + \omega(v) \geq \omega(N(v))$. By applying Reduction 1.8, u is included and its neighbors excluded from \mathcal{I} , resulting in the reduced graph on the right.

Reduction 1.8 (Almost Twin. Figure 1)

Let $u, v \in V$ be non-adjacent vertices such that $N(u) \subseteq N(v)$. If $\omega(u) + \omega(v) \geq \omega(N(v))$, then include u .

Reduced Graph	$G' = G - N[u]$
Offset	$\alpha_\omega(G) = \alpha_\omega(G') + \omega(u)$
Reconstruction	$\mathcal{I} = \mathcal{I}' \cup \{u\}$

Proof. Let $u, v \in V$ be non-adjacent vertices such that $N(u) \subseteq N(v)$ and $\omega(u) + \omega(v) \geq \omega(N(v))$. Assume there is an MWIS \mathcal{I} of G not containing u . Then, there is a vertex $x \in N(u)$ such that $x \in \mathcal{I}$ which again results in $v \notin \mathcal{I}$. We can therefore construct a new solution $\mathcal{I}' = \mathcal{I} \setminus N(v) \cup \{u, v\}$ with $\omega(\mathcal{I}') \geq \omega(\mathcal{I})$. It follows that there always exists an MWIS that includes u . ◀

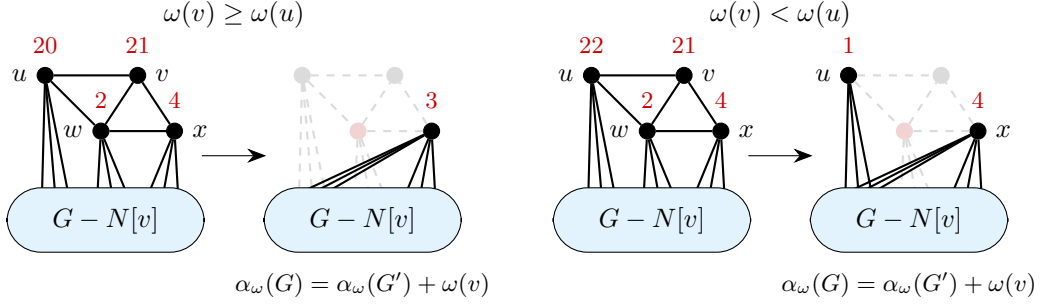
► **Remark 2.** The Reduction 1.8 can be extended as well. Instead of requiring that $\omega(u) + \omega(v) \geq \omega(N(v))$ the same reduction can also be applied if $\omega(u) + \omega(v) \geq \alpha_\omega(G[N(v)])$, since an MWIS for $N(v)$ is a subset of $N(v)$.

► **Remark 3.** Note that applying Reduction 1.5, creates exactly the pattern needed for Reduction 1.8. If the weight constraint is satisfied, u and v are almost twins and Reduction 1.8 can be applied.

Simplicial Vertex Based Reduction

Recall that a simplicial vertex v is a vertex where the neighborhood $N(v)$ forms a clique. The idea of Reduction 1.1 is that a simplicial vertex v can be included in the solution if it is of maximum weight in its neighborhood. This rule was first introduced by Lamm et al. [44]. In the following reduction we extend this idea further. Here, we consider a vertex v which is almost simplicial, meaning there is one vertex $u \in N(v)$ such that if it is removed $N(v) \setminus \{u\}$ forms a clique. We call the pattern of the two vertices $u, v \in V$ such that $u \in N(v)$ and $N(v) \setminus \{u\}$ forms a clique for a u - v -funnel.

The main idea of this reduction is that, under certain weight constraints, if u and v form a u - v -funnel either u or v is in an MWIS. In this situation, only the three following solution patterns in $N[v]$ can occur. First, the vertex v is in an MWIS. Second, the vertex u and one other neighbor $x \in N(v) \setminus N[u]$ are in the solution. For this case we need to add additional edges between the vertex u and the remaining vertices $x \in N(v) \setminus N[u]$. Third, only the vertex u is part of the solution. Note that the third case can only occur when $\omega(u) > \omega(v)$.



■ **Figure 2** Illustration for the two cases of the Weighted Funnel, Reduction 1.9.

These three cases lead to the weighted version of the funnel reduction, see Reduction 1.9. The unweighted version of this reduction was presented by Xiao et al. [66].

Reduction 1.9 (Weighted Funnel. Figure 2)

Assume $u, v \in V$ forms a u - v -funnel and that $\omega(v) \geq \max\{\omega(x) \mid x \in N(v) \setminus \{u\}\}$. Furthermore, let $N'(v) = \{x \in N(v) \setminus N[u] \mid \omega(x) + \omega(u) > \omega(v)\}$.

- If $\omega(v) \geq \omega(u)$, fold v and u into its neighborhood.

Reduced Graph $G' = G - (N[v] \setminus N'(v))$ and for all $x \in N'(v)$, let $N(x) = N(x) \cup N(u)$ and $\omega(x) = \omega(x) + \omega(u) - \omega(v)$

Offset $\alpha_\omega(G) = \alpha_\omega(G') + \omega(v)$

Reconstruction If $\mathcal{I}' \cap N(v) = \emptyset$, then $\mathcal{I} = \mathcal{I}' \cup \{v\}$, else $\mathcal{I} = \mathcal{I}' \cup \{u\}$

- If $\omega(v) < \omega(u)$, fold v into its neighborhood.

Reduced Graph $G' = G - (N[v] \setminus (N'(v) \cup \{u\}))$ with $\omega(u) = \omega(u) - \omega(v)$ and for all $x \in N'(v)$, let $N(x) = N(x) \cup N(u)$

Offset $\alpha_\omega(G) = \alpha_\omega(G') + \omega(v)$

Reconstruction If $\mathcal{I}' \cap N(v) = \emptyset$, then $\mathcal{I} = \mathcal{I}' \cup \{v\}$

Before giving the proof for the Reduction 1.9, we introduce the following lemma using the transformation of the extended weighted struction reduction introduced and proven by Gellner et al. [24]. The intuition is that for a vertex v in the graph, we can either choose v to be in the solution or some independent set in $G[N(v)]$. These independent sets are encoded as vertices connected to form a clique such that only one independent set in $G[N(v)]$ can be chosen. If the weight of an independent set in the neighborhood of v is less than the weight of v , it is not added in the transformation, since these vertices could always be swapped with v to create an equal or higher weight independent set.

► **Lemma 4.** Let $v \in V$ and C be the set of independent sets in $G[N(v)]$ with higher weight than v . Then, we can construct an instance G' by removing $N[v]$ and for each solution $c \in C$, add a vertex v_c with weight $\omega(c) - \omega(v)$. All these solution vertices are connected to form a clique. Furthermore, all v_c are connected to vertices in $N(c) \setminus N(v)$ that are adjacent to a vertex in c , but not adjacent to v . It then holds that $\alpha_\omega(G) = \alpha_\omega(G') + \omega(v)$.

Proof. Proven by Gellner et al. [24] in the extended weighted struction reduction. ◀

Proof for Reduction 1.9. Assume $u, v \in V$ forms a u - v -funnel and $\omega(v) \geq \max\{\omega(x) \mid x \in N(v) \setminus \{u\}\}$. Let $N'(v)$ be as it is defined in the reduction rule. As a first step, we prove

that an MWIS contains either u or v . Therefore, assuming u is not in an MWIS, we can exclude u , resulting in v being a simplicial vertex of maximum weight. Now, we can include v (see Reduction 1.1). In the other case, vertex u is in an MWIS. Using this, we can exclude their common neighborhood $N(v) \cap N(u)$. Since $N'(v)$ still forms a clique, only the following three cases for an MWIS \mathcal{I} in G have to be considered. First, v is in \mathcal{I} , second only u is part of \mathcal{I} and third, u and *one* of the remaining neighbors $x \in N'(v)$ is in the solution.

We now apply the graph transformation of Lemma 4 to the solutions described. Note that when the weight of the independent set is less than $\omega(v)$, no vertex is added in the transformation. In our case, this means that we can remove the remaining neighbors $x \in N'(v)$ if $\omega(x) + \omega(u) < \omega(v)$.

Furthermore, every solution including a vertex $x \in N'(v)$ has to also contain u by the weight assumption $\omega(v) \geq \omega(x)$. The vertices $x \in N'(v)$ now represent the solutions containing x and u . Therefore, all these remaining neighbors have to be connected to the neighborhood of u . By Lemma 4 it holds that $\alpha_\omega(G) = \alpha_\omega(G') + \omega(v)$.

Next, we consider the different weight relations between u and v . If $\omega(u) < \omega(v)$, there is no solution of higher weight than $\omega(v)$ that only contains u . Therefore, u is not present in the transformed graph.

Otherwise, the vertex u remains in the reduced instance. Note that in this case, there are edges connecting u to all remaining neighbors of v . For each remaining neighbor $x \in N'(v)$, its weight is increased by $\omega(u) - \omega(v)$. Afterward, we apply Reduction 1.5 to all pairs of u and an $x \in N'(v)$, which removes all edges connecting u to $x \in N'(v)$. Reduction 1.5 also reduces the weights of the vertices in $N'(v)$ by the current weight of u , which was reduced by the weight of v . This results in the original weight of the neighbors since $\omega(x) = \omega(x) + \omega(u) - \omega(v) - (\omega(u) - \omega(v))$. These steps give the reduced graph G' as described by Reduction 1.9. ◀

Extended Heavy Set Reduction

An independent set \mathcal{I} is called a heavy set, if for any independent set C in the induced subgraph $G[N(\mathcal{I})]$ it holds $\omega(N(C) \cap \mathcal{I}) \geq \omega(C)$. This concept was introduced by [65]. Using this definition, for every independent set $\tilde{\mathcal{I}}$, an equivalent or higher weight independent set \mathcal{I}^* can be constructed by $\mathcal{I}^* := \tilde{\mathcal{I}} \setminus N(\mathcal{I}) \cup \mathcal{I}$. Therefore, these vertices can always be included. We now extend the Reduction 1.4 presented by Xiao et al. [65] to the case of a heavy set of three vertices in Reduction 1.10.

Reduction 1.10 (Heavy Set 3)

Let u, v and w be vertices forming a heavy set, then include u, v and w .

<i>Reduced Graph</i>	$G' = G - N[\{u, v, w\}]$
<i>Offset</i>	$\alpha_\omega(G) = \alpha_\omega(G') + \omega(u) + \omega(v) + \omega(w)$
<i>Reconstruction</i>	$\mathcal{I} = \mathcal{I}' \cup \{u, v, w\}$

Proof. The proof follows by definition of a heavy set. ◀

Extended Unconfined Reduction

We extend the unconfined vertex reduction rule for the weighted version of MIS by Xiao et al. [64]. The intuition behind this rule is that a vertex v can be removed if a contradiction is obtained by assuming every MWIS of G includes v . To define the rule, we first introduce the following definitions and lemma.

Let S be an independent set of G . As in the original unconfined reduction, a vertex $x \in N(S)$ is called a *child* of S if $\omega(x) \geq \omega(S \cap N(x))$. For each vertex $y \in N(x) \setminus N[S]$, let $\tilde{\mathcal{I}}_y$ be the MWIS of $G[(N(x) \setminus \{y\}) \setminus N[S]]$. Unlike the original rule, here, a child is called an *extending child* if for some $y \in N(x) \setminus N[S]$ it holds that $\omega(x) \geq \omega(S \cap N(x)) + \omega(\tilde{\mathcal{I}}_y)$. Such a vertex y is called a *satellite* of S . Intuitively, a satellite is a vertex that must be included in every MWIS under the assumption that S is contained in every MWIS. If it was not, we would have the contradiction we are looking for.

► **Lemma 5.** *Let S be an independent set that is contained in every MWIS of G . Then, every MWIS also contains the satellites from each extending child x of S .*

Proof. Let S be an independent set that is contained in every MWIS of G and $x \in N(S)$ be an extending child. Assume, towards a contradiction, that there exists a satellite y that is not part of every MWIS. By definition, $\omega(x)$ is now greater or equal to $\omega(S \cap N(x)) + \omega(\tilde{\mathcal{I}}_y)$. Thus, for any MWIS that includes S but not y , we can replace $S \cap N(x)$ and $\tilde{\mathcal{I}}_y$ with x to obtain a greater or equally large independent set, which contradicts the assumption that S was contained in every MWIS of G . ◀

Reduction 1.11 (Extended Unconfined Vertices)

A vertex $v \in V$ can be removed if it is unconfined proven by the following procedure. Start with a set $S = \{v\}$. We assume S is contained in every MWIS in G . We can search for a contradiction by repeatedly extending S with satellites from one extending child until one of the following conditions hold

1. There exists a child x such that $\omega(x) \geq \omega(S \cap N(x)) + \alpha_\omega(G[N(x) \setminus N[S]])$.
2. There exist no further satellites to extend S .

In the second case, the set S confines v , meaning every maximum weight independent set that contains v , also contains S and we can not remove v . In the first case, v is called *unconfined* and can be excluded.

Reduced Graph	$G' = G - v$
Offset	$\alpha_\omega(G) = \alpha_\omega(G')$
Reconstruction	$\mathcal{I} = \mathcal{I}'$

Proof. Assume that S , initially just $\{v\}$, is contained in every MWIS and that Condition 1 holds. By Lemma 5, after every extension of S with satellites, S is still contained in every MWIS in G . But when Condition 1 holds, any MWIS \mathcal{I} of G with $S \subseteq \mathcal{I}$ can be modified using the child x to obtain a new independent set $\mathcal{I}' = \{x\} \cup (\mathcal{I} \setminus N(x))$. From Condition 1, it follows that $\omega(\mathcal{I}') \geq \omega(\mathcal{I})$, breaking the assumption that S is contained in every MWIS of G . Therefore, v is removable. ◀

► **Remark 6.** This extended version of unconfined was already suggested in a remark by Xiao et al. [65], but they did not introduce it formally as is done here. It is also important to note that this version of unconfined is not practical in its most general form. Several MWIS problems need to be solved for each extending child, making it too computationally intensive for practical implementations. We implement this rule by restricting it to only search for satellites in neighborhoods that form an independent set. This way, we can detect multiple satellites from an extending child without solving any additional MWIS problems.

4.2 GNN Models

In the following, we introduce a new method for screening when to apply data-reductions based on Graph Neural Networks (GNN). We also provide a new and openly available supervised-learning dataset with graphs and labeled vertices for each reduction rule. For each expensive reduction rule used in the preprocessing, a pre-trained GNN model will limit the set of vertices that should be checked for using the reduction rule. GNNs are recent additions to the field of artificial intelligence that bring successful ideas from conventional deep learning to the irregular structure of graphs [63]. Where traditional deep learning focuses on structured input, such as the grid of pixels in an image, GNNs accept the unstructured data of a graph.

As a first stage of this task, we evaluate the most popular GNN architectures used in combinatorial optimization, namely Graph Convolutional Network (GCN) [40] and Graph Sample and Aggregate (GraphSAGE) [32]. In addition to GCN and GraphSAGE, we also introduce a slightly altered GNN architecture, which we name the LEARNANDREDUCE-MODEL (LR). At a high level, these GNN architectures combine conventional neural networks with message passing. In this *message passing*, every vertex sends messages to its neighbors and aggregates the received messages. One iteration of message passing and a neural network transformation makes up a GNN *layer*. Several of these layers are stacked on top of each other to make up a GNN model. The goal is that after these message-passing layers, the final vertex embedding can be used to estimate how likely it is that a reduction rule will succeed at this vertex.

An undirected graph $G = (V, E, H)$ is given as input to the model, where H is the initial feature representation for the vertices in the graph. Any number of vertex features can be used. Using the vertex weight is an obvious choice, but additional features such as vertex degrees and local clustering coefficients are common [47]. Note that computing complicated features for the vertices can add significant computational overhead to the model, which is important for our application since running the model should not take longer than checking the reduction rules. This feature representation will change after each layer in the model. For a vertex $u \in V$ at layer l , the feature representation is denoted by $H_u^{(l)}$. The length d of the feature vector at layer l is denoted by $d^{(l)}$. Stacking all the feature vectors at the l 'th layer gives the matrix $H^{(l)} \in \mathbb{R}^{|V| \times d^{(l)}}$. Independent from any input graph, every layer in the GNN model has trainable parameters $W^{(l)}$, bias $b^{(l)}$, and a non-linear activation function σ . Every model uses the $\text{ReLU}(x) := \max(0, x)$ activation function for internal layers and $\text{Sigmoid}(x) := \frac{1}{1+e^{-x}}$ for the output layer. Note that these activation functions are applied element-wise when the input is a vector. With this, we define each model used for testing.

Graph Convolutional Network

The GCN architecture was the first successful extension of convolutional neural networks to work directly on graphs. At each layer in a GCN model, every node aggregates information from its immediate neighbors and combines it with its own data. After this, the information stored in each node is passed through the layer-specific neural network to create the node information for the next layer. The layer-wise propagation rule can be seen in Algorithm 1. Note that the GCN model assumes that there are self-edges added to the input graph. If not, a vertex will not include its own feature representation in the neighborhood aggregation.

■ **Algorithm 1** GCN propagation rule. Self edges are added to the input graph and T_u is a temporary variable holding the aggregated feature vectors of the neighbors of u .

```

1 for  $u \in V$  do
2    $T_u \leftarrow \sum_{v \in N(u)} H_v^{(l)} / \sqrt{|N(v)|}$ 
3    $H_u^{(l+1)} \leftarrow \sigma(W^{(l)} \cdot T_u + b^{(l)})$ 
4 end

```

Graph Sample and Aggregate

GraphSAGE expands on GCN in two notable ways. First, it can use any differentiable aggregation function, such as aggregating the neighborhood based on mean, max, sum, or even more complicated functions, such as a long short-term memory (LSTM) machine-learning model. Second, GraphSAGE concatenates the feature vector of a vertex with the aggregated information from its neighborhood. This is in contrast to the self-edges of the GCN and allows information to skip from one layer to the next without going through the neighborhood aggregation. The general layer-wise propagation rule can be seen in Algorithm 2.

■ **Algorithm 2** GraphSAGE propagation rule. T_u is a temporary variable holding the aggregated feature vectors of the neighbors of u .

```

1 for  $u \in V$  do
2    $T_u \leftarrow \text{AGGREGATE}(\{H_v^{(l)} \mid v \in N(u)\})$ 
3    $H_u^{(l+1)} \leftarrow \sigma(W^{(l)} \cdot \text{CONCAT}(H_u^{(l)}, T_u) + b^{(l)})$ 
4 end

```

Learn and Reduce

The proposed LEARNANDREDUCE (LR) architecture differs slightly from the GCN and GraphSAGE architectures. Instead of applying the weighted transformation after the aggregation, it is applied during the neighborhood aggregation. Algorithm 3 gives the exact layer-wise propagation rule. To give an intuition for why this approach could learn reduction rules better than GCN and GraphSAGE, consider the case of the extended single-edge reduction. For this reduction rule, we are looking for two adjacent vertices $u, v \in V$ such that $\omega(v) \geq \omega(N(v)) - \omega(u)$. For more information on this reduction rule, see Table 1 or Gu et al. [29]. Assuming the node weights and neighborhood weights are given as input features, the LR architecture could conceivably detect this pattern during the first layer of the model since the concatenated feature representation of u and v would contain all the necessary information to decide if the rule can be applied. In contrast, GCN and GraphSAGE would aggregate the entire neighborhood before the first weighted transformation, potentially obscuring the necessary information required to make the correct prediction. Note that this is not a novel GNN architecture and could arguably fit into the GraphSAGE framework.

■ **Algorithm 3** LEARNANDREDUCE propagation rule. The main difference with this architecture compared to GCN and GraphSAGE is the use of weighted transformation during neighborhood aggregation.

```

1 for  $u \in V$  do
2    $H_u^{(l+1)} \leftarrow \text{MEAN}(\{\sigma(W^{(l)} \cdot \text{CONCAT}(H_u^{(l)}, H_v^{(l)}) + b^{(l)}) \mid v \in N(u)\})$ 
3 end

```

4.3 Training Data Generation

The supervised-learning dataset contains each instance twice, first the original instances without any reductions applied, and second the same instance after applying a set of fast reductions. These fast reductions are not considered relevant for early screening because they are so computationally cheap that we would always check them exhaustively. A comprehensive list of these reductions is given in Table 1. We refer to these two versions of the same instance as ORIGINAL and REDUCED. The truth labels for each reduction rule are generated by testing the rule on each vertex without performing the reduction in the successful case. This way, each label is created using a clearly defined procedure without ambiguity. For the most costly reduction rules that rely on solving MWIS instances in subgraphs, a third class is used in the case of a timeout event. This gives the following labeling for each combination of a vertex and reduction rule.

$$\text{LABEL}(v) = \begin{cases} 0 : \text{Unsuccessful reduction} \\ 1 : \text{Successful reduction} \\ 2 : \text{Timeout} \end{cases}$$

It is not always clear what vertex should be labeled as successful, especially for reductions where the rule starts from one vertex but ends up reducing another. It would be easiest if the starting vertex always received the successful label, given that the purpose of the trained model is to perform early screening. However, this would make the task of learning the rules unnecessarily hard for some reduction rules. The complete list of reduction rules used and how the labels are generated can be seen in Table 1. Note that the labeled vertices are always chosen to make the training as simple as possible. For example, the heavy set reduction starts from a source vertex and looks for two vertices in the neighborhood that can be included. If the successful labels were placed on the source vertices, the model would need to detect vertices adjacent to two vertices likely to be part of a solution. In contrast, if the labels are placed on the heavy vertices themselves, the pattern is simply to detect vertices that are likely part of a solution. We can still use the trained model for screening, but instead of deciding what vertices to start the reduction from, we only use suggested vertices from the neighborhood of the source vertex.

4.4 The Learn and Reduce Approach

In the following, we describe our LEARNANDREDUCE approach in more detail. In addition to our new reduction rules, we also use several data reduction rules introduced by [13, 29, 24, 65]. The survey by Großmann et al. [28] presents a comprehensive collection of known reduction rules, and we enumerate them in the same way here. The complete list and a short description of each can be seen in Table 1. The most costly reduction rules, the ones below the bold line in the center of Table 1, are the ones that undergo early GNN screening before applying them. Each reduction rule will have its own pre-trained GNN model for early screening. Since we use the Sigmoid activation function, the output from the GNN will be a real number in the range from zero to one. If the GNN prediction for a vertex is greater than 0.5, that vertex will be checked using the reduction rule for which the model was trained.

The LEARNANDREDUCE reduction procedure maintains a queue of vertices to check for each reduction rule. The reduction rules are ordered based on complexity, and each rule is only checked when all the queues of easier reductions are empty. The ordering is the same as shown in Table 1, except for Reduction 1.6 which is applied before Reduction 2.5. Even if it is more expensive, it yielded better results in our tests to place Reduction

6.8 before applying the struction approach introduced by Gellner et al. [24]. An outline of how the LEARNANDREDUCE reduction procedure works is shown in Algorithm 4. Each queue is initialized with all the vertices from the graph. Whenever a successful reduction occurs, the adjacent vertices that saw a change in their neighborhood are queued up again for every reduction. This way, the reduction procedure will always return to the easier reductions as soon as possible. The vertices are not ordered within the queues beyond the first-in, first-out principle. Reduced vertices may still reside in other queues but are ignored when they are popped from the queue.

■ **Algorithm 4** The LEARNANDREDUCE reduction procedure.

Data: Graph $G = (V, E, \omega)$, set of reductions R , and set of GNN models M
Result: Reduced instance G

```

1  $i \leftarrow 0$ 
2  $Q \leftarrow \{\{0, 1, \dots, |V| - 1\} \cdot |R|\}$  /* Initialize FIFO queues for each rule */
3 while  $i < |R|$  do
4   if  $Q[i] = \emptyset$  then
5      $i \leftarrow i + 1$ 
6     /* With the Initial/Initial-Tight configurations, the next If
7      statement is changed accordingly */
8     if  $i < |R|$  and  $Q[i] \neq \emptyset$  and  $M[i]$  exists then
9        $Q[i] \leftarrow \emptyset$ 
10       $P \leftarrow M[i](G)$ 
11      for  $v \in V$  such that  $P[v] > 0.5$  do
12         $push(Q[i], v)$ 
13      end
14    end
15  else
16     $v = pop(Q[i])$ 
17    if  $v$  is not reduced then
18       $G' \leftarrow R[i](G, v)$  /* Try reduction on  $v$  */
19      if  $G' \neq G$  then
20         $G \leftarrow G'$  /* Successful reduction */
21         $i \leftarrow 0$ 
22        for each changed vertex  $u \in V$  and  $q \in Q$  do
23          if  $u \notin q$  then
24             $push(q, u)$ 
25          end
26        end
27      end
28    end
29  end

```

There are multiple ways to incorporate the GNN screening. As reduction rules are applied, the graph continuously changes. Predictions made at the start of the reduction procedure might not be relevant later. Therefore, we propose three GNN screening configurations.

Always

In this configuration, the queue for each expensive reduction is only checked to see if it is non-empty. If that is the case, the queue is always replaced by new suggestions from the GNN model. This means the GNN model could be evaluated multiple times during the reduction process.

Initial

Instead of always evaluating the GNN model, the Initial configuration only evaluates the GNN model the first time the rule is used. Recall that each queue is initialized with all the vertices in the graph, meaning that the first time the rule is used is also when the potential screening effect is the highest. After this initial screening, the reduction rule goes back to working as without GNN screening, meaning if further reductions occur and vertices are added back to the queue, then these will be checked exhaustively.

Initial Tight

Again, the GNN model is only evaluated the first time the reduction rule is used. However, instead of returning to the normal queue-based application afterward, the queue cannot accept any additional vertices. This means that the initial suggestions from the GNN model are the only vertices that will be checked using that reduction rule. Intuitively, this configuration is the most aggressive form of early screening and will take the least time.

For two reductions, namely Reduction 6.8 Critical Set and Reduction 6.6 Cut Vertex, the queue base approach does not fit so well. The Critical Set reduction needs to construct a new bipartite graph and compute the maximum flow, and the Cut Vertex reduction needs to find all articulation points. Therefore, it is natural to apply these reductions globally. Regarding the reduction queues, these two reductions still have the same queues as the other reductions. However, as long as the queue is non-empty, the reduction is applied globally, and the entire queue is cleared afterward. This also extends to the GNN screening, but we only apply the reduction globally if the GNN suggests applying the rule on more than 1% of the graph.

5 The CHILS Algorithm

The proposed heuristic consists of two parts: (1) a simple iterated local search procedure we refer to as BASELINE, and (2) a new, concurrent heuristic called CHILS (Concurrent Hybrid Iterated Local Search). In the following section, we first give a high-level overview of the proposed approach and then provide a detailed description of each component of our heuristic.

5.1 High-Level Description

An uncomplicated heuristic implemented very efficiently is often better in practice than a complicated one that runs slowly, especially when the heuristic makes heavy use of random decisions. This can be seen from the results of programming competitions such as PACE (Parameterized Algorithms and Computational Experiments), where fast randomized local search has become the default heuristic strategy among the winning solvers [38, 26, 10]. Note that the PACE competition setting restricts the time to solve the problem. We also used this approach for our baseline local search. First, randomly alter a local area in the current

■ **Table 1** The full list of reductions used in LEARNANDREDUCE along with a brief description of each one. The id’s are taken from [28]. The last two columns connect the reduction rules to the supervised-learning dataset. Note that we often combine similar reduction rules for the dataset. The bold vertical line in the center of the table indicates the distinction between cheap and expensive reduction rules.

Id	Name	Brief Description	Data Name	Label
2.2	Neighborhood Removal [44]	Includes a vertex v if $\omega(v) \geq \omega(N(v))$	Neighborhood Removal	Included vertex
1.1	Degree One [29]	Reduces or folds all degree-one vertices	Degree-One	Degree-one vertex
1.2	Triangle [29]	Reduces degree-two vertices with adjacent neighbors	Degree-Two	Degree-two vertex
1.3	V-Shape [44, 29]	Reduces degree-two vertices with non-adjacent neighbors		
3.1	Simplicial Vertex [44]	Includes a vertex v if $N(v)$ forms a clique and $\omega(v) \geq \max_{u \in N(v)} \omega(u)$	Clique	Simplicial vertex
3.2	Simplicial Weight Transfer [44]	Folds a vertex v if $N(v)$ forms a clique and $\omega(v) \leq \max_{u \in N(v)} \omega(u)$		
4.1	Domination [44]	Exclude a vertex that dominates a lighter vertex	Domination	Excluded vertex
4.2	Basic Single Edge [29]	Exclude a vertex v if for some vertex $u \in N(v)$, $\omega(N(u) \setminus N(v)) \leq \omega(u)$	Single Edge	Excluded vertex
4.3	Extended Single Edge [29]	For $\{u, v\} \in E$, exclude $N(u) \cap N(v)$ if $\omega(v) \geq \omega(N(v)) - \omega(u)$	Extended Single Edge	Excluded vertices
7.1	Twin [44]	Limited to independent neighborhood	Twin	Both twins
New	Extended Twin	Fold or reduce all twins		
New	Almost Twin	Includes a vertex v if for some non-adjacent u , $N(v) \subseteq N(u)$ and $\omega(v) + \omega(u) \geq \omega(N(u))$	Almost Twin	Included vertex
New	Weighted Funnel	For $\{u, v\} \in E$ with $\omega(v) = \max\{\omega(w) : w \in N(v) \setminus \{u\}\}$ and $N(v) \setminus \{u\}$ forms a clique, we can fold or reduce parts of $N(v)$	Funnel	Almost simplicial vertex
2.3	Clique Neighborhood Removal [44]	Extension of Reduction 2.2 for cliques in the neighborhood of v	—	—
New	Extended Domination (Reverse)	For $\{u, v\} \in E$ with $N[u] \subseteq N[v]$ and $\omega(u) < \omega(v)$, remove $\{u, v\}$ and set $\omega'(v) = \omega(v) - \omega(u)$	—	—
New	Extended Unconfined	Exclude a vertex v if a contradiction is obtained by assuming v is part of every MWIS	Unconfined	Excluded vertex
6.8	Critical Weight Independent Set [13]	Included the vertices of a (possibly empty) independent set \mathcal{I}_c such that $\omega(\mathcal{I}_c) - \omega(N(\mathcal{I}_c)) = \max\{\omega(\mathcal{I}) - \omega(N(\mathcal{I})) : \mathcal{I} \text{ is an IS of } G\}$	Critical Set	Included vertices
5.4	Extended Reduced Structon [24]	A vertex v and its neighborhood can be transformed into a clique where each vertex represents an independent set in $N[v]$	—	—
2.5	Generalized Neighborhood Folding [44, 1]	Extension of Reduction 2.2 with solving the MWIS in the neighborhood of v	Generalized Fold	Included vertex
2.7	Heavy Set [65]	Finds a pair of vertices that can be included based on their combined neighborhoods	Heavy Set	Included vertices
New	Heavy Set 3	Extension of Reduction 2.6 for three vertices instead of two	Heavy Set 3	Included vertices
6.6	Cut Vertex [64]	Fold or reduce an articulation point v along with the smaller component in $G - v$	Cut Vertex	Articulation points

solution. Then, apply greedy improvements in random order until a local optimum is found. Finally, if the new local optimum is worse than the previous, backtrack the changes and repeat. Compared to more complicated heuristics, the main benefit of our BASELINE heuristic is that it is inherently local. Regardless of the graph size, one iteration of the search will typically only touch vertices a few edges away from where the random alteration started. Backtracking to the best solution is also local, as long as queues are used to track changes. Using queues also differentiates our BASELINE from other heuristics, such as HILS [52], that make a copy of the entire solution instead.

The high-level idea of CHILS is a new metaheuristic we call CONCURRENT DIFFERENCE-CORE HEURISTIC. Instead of only trying to improve one solution, we maintain several and update each one concurrently. At fixed intervals, the solutions are used to create a DIFFERENCE-CORE (D-CORE) instance based on where the solutions differ. In other words, if a vertex is part of all or none of the solutions, it will not be part of the D-CORE. The intuition is that the intersection of the solutions is likely to be part of an optimal solution, and where they differ indicates areas where further improvements could be made. Since there is no guarantee that the intersection of the solutions is part of an optimal solution, the CONCURRENT DIFFERENCE-CORE HEURISTIC alternates between looking for improvements on the original instance and the D-CORE, where the D-CORE is always constructed according to the current solutions. While the general CONCURRENT DIFFERENCE-CORE HEURISTIC can work using any heuristic method, our CHILS heuristic uses the BASELINE iterated local search.

5.2 Baseline Local Search

The outline of the baseline local search is shown in Algorithm 5. Each search iteration starts by picking a random vertex u from the graph. If the vertex is already in the solution $u \in S$, or the tightness of u is one, i.e. $|N(u) \cap S| = 1$, then an alternating augmenting path (AAP) is used to perturb the current solution. If u is not currently in the solution, it is added along with a random number of additional changes in its close proximity. The vertices that see a change in their neighborhood are considered “close proximity” to u . These vertices are continuously queued up in Q to find greedy improvements more efficiently later. We also use the size of Q to control the amount of random changes. We stop perturbing the solution once $|Q|$ exceeds m_q , where m_q is a hyperparameter for the BASELINE heuristic. The benefit of using Q and m_q is that it stabilizes the computational cost for one iteration across different graph densities. For instance, the number of changes needed to fill Q in a dense area will be higher than in a sparse area.

After perturbing the current solution, greedy improvements are made to find a new local optimum. Having the queue Q of candidate vertices helps speed up the search for this new local optima. We incorporate three greedy improvement operators for GREEDY in BASELINE described in the following.

Neighborhood Swap

For a vertex $u \notin S$, if $\omega(u) > \omega(N(u) \cap S)$, then the independent set obtained by inserting the vertex u and removing all neighbors of u that are currently in the solution, i.e. $S = \{u\} \cup (S \setminus N(u))$, leads to an independent set of higher weight. The total sum of the weights of each neighbor currently in the solution $\sum_{v \in (N(u) \cap S)} w(v)$ is maintained at all times. This additional data structure allows the neighborhood swap to be checked in $\mathcal{O}(1)$ time.

Algorithm 5 Baseline Local Search

Data: Graph $G = (V, E, w)$, independent set S , max queue size m_q , and time limit t
Result: Improved independent set S

```

1  $Q \leftarrow \emptyset$  /* Always filled with vertices that observe changes to  $S$  */
2 while time spent  $< t$  do
3    $\text{cost} \leftarrow \omega(S)$ 
4    $u \leftarrow$  uniform random from  $[0, |V| - 1]$ 
5   if  $u \in S$  or  $|N(u) \cap S| = 1$  then
6     |  $\text{AAP-moves}(G, S, u)$ 
7   else
8     |  $S = \{u\} \cap S \setminus N(u)$ 
9     | while  $|Q| < m_q$  do
10    | |  $v \leftarrow$  random element from  $Q$ 
11    | | if  $v \in S$  then
12    | | |  $S = S \setminus \{v\}$ 
13    | | else
14    | | |  $S = \{v\} \cap S \setminus N(v)$ 
15    | | end
16    | end
17   end
18    $\text{GREEDY}(G, S, Q)$ 
19   if  $w(S) < \text{cost}$  then
20     | undo changes to  $S$ 
21   end
22 end
23 return  $S$ 

```

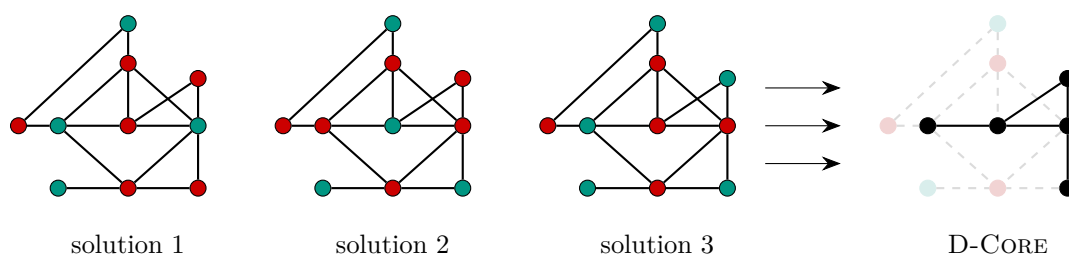
Two-One Swap

For a vertex in the current solution $u \in S$, consider the set $T = \{v \in N(u) \mid N(v) \cap S = \{u\}\}$ with vertices in the neighborhood of u whose only neighbor included in the solution is u . If there exists a pair of vertices $\{x, y\} \subseteq T$ such that $\{x, y\} \notin E$ and where $w(u) < w(x) + w(y)$, then swapping u for x and y leads to a better solution. Examining all two-one swaps can be done in $\mathcal{O}(|E|)$ [7].

Alternating Augmenting Path

An alternating augmenting path (AAP) is a sequence of vertices that alternate between being in and out of the solution S . AAP moves are used both for perturbation and finding greedy improvements. When used for perturbation, the AAP is always extended in a random direction. After no more vertices can be added to the path, the entire AAP is applied to the solution unless a strictly improving prefix of the path exists. When searching for greedy improvements, the path always starts from a one-tight vertex and extends in the best direction possible.

We use a slightly modified version of the AAP introduced by Dong et al. [18]. Let U be the set of vertices on the AAP in S , and \bar{U} be the vertices on the AAP not in S . A valid AAP has the property that the set S' obtained by applying the AAP, i.e. $S' = (S \setminus U) \cup \bar{U}$ is also an independent set. This means \bar{U} must also be an independent set where $N(\bar{U}) \cap S = U$.



■ **Figure 3** Illustration for the D-CORE. Vertices that are part of all or non of the solutions are not part of the D-CORE.

The main purpose of APPs is to find improving paths where $\omega(\bar{U}) > \omega(U)$, and swap the vertices in U for those in \bar{U} to obtain a heavier independent set. As a secondary use case, they can also perturb the current solution. The benefit of using AAPs instead of random perturbation is that the cardinality of the new solution can only be one worse than the original. Constructing an APP starts with either a single vertex $u \in S$ or a pair of vertices $v \notin S, u \in S$, such that $N(v) \cap S = \{u\}$. The AAP is then extended from the last vertex u on the path two vertices $x \in N(u), y \in N(x)$ at a time, such that the following three conditions are met:

1. x is not adjacent to any vertices in \bar{U}
2. x is not currently in \bar{U}
3. x is adjacent to precisely two vertices in the solution $N(x) \cap S = \{u, y\}$

Notice that y is allowed to already be on the path. In this scenario, after applying the AAP to S , x would not have neighbors currently in the solution. This is the main difference to the definition of AAP given in [18].

5.3 CHILS

We give an overview of our concurrent heuristic CHILS in Algorithm 6. First, we run BASELINE P times, with a time limit of t_G seconds, on the full graph with different seeds and slightly modified Q values to increase the randomness. We assign each of the computed solutions an *id* and always keep track of the best solution found so far. This solution will only be modified if a better solution is found. Note that the id of the best solution can change during the algorithm’s execution time. After the runs on the full graph are finished, i.e. after $P \times t_G$ seconds, we construct the D-CORE instance. This is done by removing vertices that are part of all or none of the P independent sets, see Figure 3 for an example.

On the D-CORE, we again start our baseline local search P times with a time limit of t_G to generate new solutions. An independent set computed on the D-CORE can replace the previous solution with the same id. However, for solutions with an even id as well as for the best solution found so far, replacements are only made if the D-CORE solution is of higher weight. Letting half of the solutions always accept the D-CORE solution helps diversify the search.

Using the D-CORE helps concentrate the local search on the “more difficult” regions of the graph, where our P solutions differ. However, since the areas where they agree are not necessarily part of an optimal solution, CHILS alternates between using the BASELINE on the original instance and the recomputed D-CORE based on the current P solutions.

If the number of vertices in the D-CORE falls below some small constant value, it indicates that the P solutions are all quite similar. Since this reduces the benefit of our

Algorithm 6 The CHILS Algorithm

Data: Graph $G = (V, E, \omega)$, number of solutions P , max queue size m_q , time limit for the full graph t_G , time limit for the D-CORE t_C , and overall time limit t

Result: Independent set S

```

1  $C = \{S_1, S_2, \dots, S_P\}$  /* using GREEDY( $G, \emptyset, V$ ) with different seeds */
2 while time spent <  $t$  do
3   parallel for  $S_i \in C$  do
4      $S_i = \text{BASELINE}(G, S_i, m_q + 4i, t_G)$ 
5   end
6    $G' \leftarrow$  compute D-CORE using  $C$ 
7   parallel for  $S_i \in C$  do
8      $S' = \text{BASELINE}(G', \emptyset, m_q + 4i, t_C)$ 
9     if  $\omega(S') + \text{offset} \geq \omega(S_i)$  OR ( $i$  is odd AND  $S_i$  is not best) then
10      apply  $S'$  to  $S_i$ 
11    end
12  end
13  if  $|V'| < 500$  then
14    PARALLEL_PERTURBE( $C$ )
15  end
16 end
17 return  $S \in C$  with largest weight

```

approach, we perturb all solutions with an odd id, except for the best solution, and without backtracking in the case where the new local optima is worse. In Algorithm 6, this is shown as PARALLEL_PERTURBE on line 14, where perturbing one solution is done as described in lines 9-16 of Algorithm 5. As with accepting replacement solutions from the D-CORE, perturbing only half the solutions here helps to diversify the search and escape local optima.

Parallel CHILS

Our CHILS approach is easily parallelizable, with a natural choice for the number of solutions being exactly the number of cores available on the machine, allowing each solution to be improved simultaneously. In this configuration, the worst-case scenario will be similar to running the underlying BASELINE sequentially, at least when technical details such as memory bandwidth and dynamic clock speeds are ignored. For larger numbers of solutions, P should be divisible by the number of threads running to ensure that no threads are idle.

6 Experimental Evaluation

The following section introduces the experimental setup and establishes the datasets used for evaluating the proposed approaches. Then, we present GNN training results, preprocessing results, and finally state-of-the-art comparison for BASELINE and CHILS.

6.1 Methodology

All the experiments were run on a machine with an Intel Xeon w5-3435X 16-core processor and 132 GB of memory, running Ubuntu 22.04.4 with Linux kernel 5.15.0-113. Both CHILS and BASELINE were implemented in C and compiled with GCC version 11.4.0 using the

-O3 flag. OpenMP is used for the parallel implementations. We evaluate eight instances in parallel for the sequential experiments. To ensure fairness between the algorithms, the instances start in the same order for each code, and only one program is evaluated at a time. We evaluate each program once for each instance.

We compare our algorithms BASELINE and CHILS to the state-of-the-art heuristic algorithms HTWIS presented in [29] by Gu et al., the hybrid iterated local search HILS by Nogueira et al. [52], the memetic algorithm $M^2WIS + s$ by Großmann et al. [27], the new metaheuristic METAMIS by Dong et al. [18], and the Bregman-Sinkhorn algorithm BSA by Haller and Savchynskyy [30]. The first three, HTWIS, HILS, and HILS, were all used in their default configurations. The source code for METAMIS is not publicly available, and therefore, we had to use the numbers reported in [18]. They used the Amazon Web Service r3.4xlarge compute node running Intel Xeon Ivy Bridge Processors and wrote the implementation of their heuristic in Java. They also run their algorithm five times with different seeds and report the best solution found. For the Bregman-Sinkhorn algorithm BSA, we use the variation that produces integer solutions only after reaching 0.1% relative duality gap for the LP relaxation by recommendation from the authors [31]².

For the comparison of different algorithms we use performance profiles [17]. At a high level, performance profiles show the relationship between the solution size or running time of each algorithm and the corresponding result produced by the competing algorithms. The performance profile gives each algorithm a non-decreasing, piecewise constant function. In general, the y-axis represents the fraction of instances where the objective function is better than or equal to τ times the best objective function value. For our solution quality comparison the y-axis shows the fraction of instances $\#\{\text{weight} \geq \tau * \text{best}\} / \#G$. Here, “weight” refers to the independent set weight computed by an algorithm on an instance, and “best” corresponds to the best result among all the algorithms shown in the plot. $\#G$ is the number of graphs in the dataset. The parameter τ is plotted on the x-axis. For maximization problems we have $0 < \tau \leq 1$. When considering performance profiles comparing running time, the y-axis displays the fraction of instances where the time taken by an algorithm is less than or equal to τ times the time taken by the fastest algorithm on that instance, more formally $\#\{t \leq \tau * \text{fastest}\} / \#\text{instances}$. Here, “t” represents the time taken by an algorithm on an instance, and “fastest” refers to the time taken by the fastest algorithm on that specific instance. As we want to minimize the time, we have $\tau \geq 1$. In the plots, we refer to these y-axes by “Fraction of instances”. In general, algorithms are considered to perform well if a high fraction of instances are solved within a factor of τ as close to 1 as possible, indicating that many instances are solved close to or better/faster than the optimum/fastest solution found by all competing algorithms.

6.2 Datasets

We use two different sets of instances for our experiments. The first set of instances consists of graphs used in previous studies. We started with all the instances used by Gellner et al. [24] and Gu et al. [29]. Our set also consists of large social networks from the Stanford Large Network Dataset Repository (snap) [48]. Additionally, we added real-world graphs from OpenStreetMaps (osm) [2, 11, 14]. Furthermore, as in Gu et al. [29] we took the same six graphs from the SuiteSparse Matrix Collection (ssmc) [3, 16] where weights correspond

² The exact command we used was `mwis_json -l temp_cont -B 50 --initial-temperature 0.01 -g 50 -b 100000000 -t [seconds] [instance]`

to population data. Each weight was increased by one, to avoid a large number of nodes assigned with zero weight. Additionally, we used instances from dual graphs of well-known triangle meshes (mesh) [56], as well as 3d meshes derived from simulations using the finite element method (fe) [58]. For unweighted graphs, we assigned each vertex a random weight that is uniformly distributed in the interval $[1, 200]$. Overall this results in 207 graphs from which we exclude instances which were already reducible by simple and fast reduction rules³, resulting in a set of 83 graphs listed in Table 10 in the Appendix.

Our second set of instances consists of 37 vehicle routing instances as used by Dong et al. [19], see Table 11 in the Appendix. Initial warm-start solutions derived from the application and clique information for the graphs are also provided for these instances. The clique information is a clique cover of the graph, i.e. a collection of potentially overlapping cliques that cover the entire graph. METAMIS [18] and BSA [30] use this clique information in their algorithms.

The early reduction screening dataset consists of the same instances as our first dataset without removing the reducible ones. There are 207 instances in the ORIGINAL instances and 71 REDUCED graphs. The difference between the number of REDUCED graphs and the 83 graphs listed in Table 10 is due to the slight difference in reduction rules used to generate these two reduced sets. This dataset will be made publicly available.

6.3 Training Results

We evaluate three GNN architectures on our new supervised learning task: GCN, GraphSAGE, and LR. Each architecture is configured to have a similar number of layers, parameters, and running time. We use two message-passing layers, followed by two layers of only weighted transformation. The input to the final two layers is a concatenation of all intermediate feature vectors, including the input features. The size of each intermediate feature vector is 16, and the size of the input vector is 8. The activation function ReLU is used for internal layers, and Sigmoid is used for the output layer. After each message passing layer, we perform random dropout with a probability of 0.2 during training. We use weighted binary cross entropy loss for loss function to adjust for the rarity of vertices labeled as successful. The weight is set exactly to the ratio between successful and unsuccessful labels in the training set. Finally, the Adam optimizer [39] is used with its default hyperparameters and 0.001 learning rate. The input features for one vertex are as follows.

1. Node weight
2. Neighborhood weight
3. Minimum neighborhood weight
4. Maximum neighborhood weight
5. Node degree
6. Average neighborhood degree
7. Minimum neighborhood degree
8. Maximum neighborhood degree

It is important to note that these reduction rules can mostly be checked in polynomial time already. Therefore, it would defeat the purpose of early screening if the screening took

³ We excluded instances which were fully reduced by running the following reductions, numbered as in [28], in the given order: Reduction 2.2, Reduction 1.1, Reduction 1.2, Reduction 1.3, Reduction 3.1, Reduction 4.1, Reduction 4.2, Reduction 4.3, Reduction 1.7, Reduction 1.8, Reduction 1.9, Reduction 2.3, Reduction 1.5, Reduction 5.4 (without blow up)

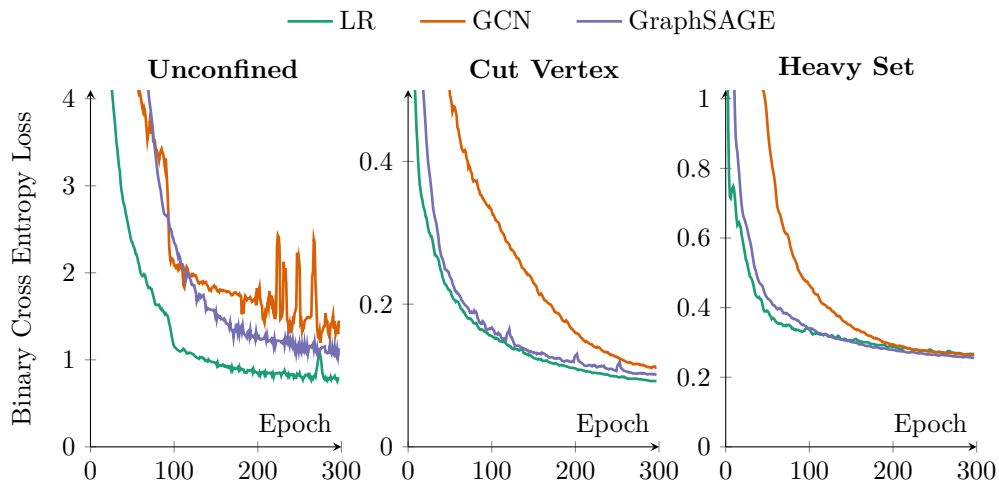
more time than the ensuing reduction. For this reason, the models are kept as small as possible. The choice of 16 internal features is made based on the fact that BLAS kernels typically need at least 16 times 4 elements at single precision to utilize the CPU fully. In other words, going any lower than 16 would reduce the efficiency at which we can perform the necessary computations. For more information, we refer the reader to [25].

For the task of early reduction screening, we are only interested in the REDUCED graphs, i.e. the graph after applying the inexpensive reductions. There are 71 REDUCED graphs in total, with over 1 million labeled vertices combined. Each graph in the dataset is divided into three parts: (1) a training set containing 60% of the vertices, (2) a validation set containing 20%, and (3) a test set containing the last 20%. Vertices labeled as 2 (timeout) are not used during training or validation. Each model is trained for 300 iterations, where one iteration uses the entire dataset.

The training data can be considered a single large graph since we split the data in terms of vertices, not individual graphs. While this graph is derived from the same instances we use to evaluate LEARNANDREDUCE later in the experiments, we argue that this is not an issue for the evaluation. First, the REDUCED graphs are snapshot images of how the instances looked after running a specific set of reductions. At inference, reductions are applied continuously as reducible vertices are found. This already means the inputs the GNN models will see at inference could be completely different from those seen during training. Furthermore, the reductions that lead to the REDUCED graphs are also not the same ones used in LEARNANDREDUCE, and all the training results are given for the test set, which is a completely different set of vertices not seen during training.

In addition to the loss value, we also provide three additional metrics from the training procedure that indicate how well the trained model will perform at early reduction screening.

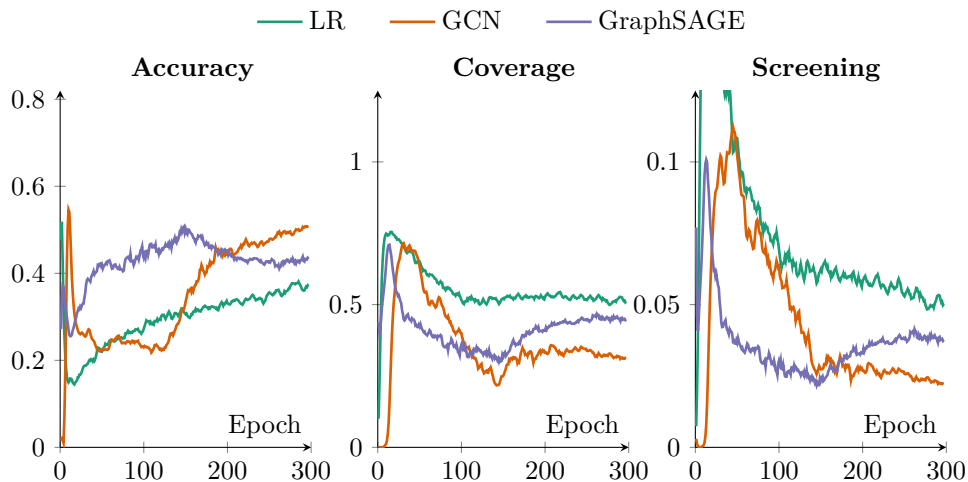
- **Accuracy** The probability that a suggested vertex can be reduced. Higher is better.
- **Coverage** The fraction of reducible vertices suggested by the model. Higher is better.
- **Screening** The fraction of the total vertices in the graph suggested. Lower is better.



■ **Figure 4** Training loss for each architecture using the unconfined, critical set, and generalized fold reduction rules on the test set. Note that the scaling of the y-axes differ.

The detailed results for the reductions Unconfined, Cut Vertex, and Heavy Set can be seen in Figure 4. The proposed LR architecture clearly outperforms the GCN and GraphSAGE for the unconfined rule, but the difference is less noticeable for the critical and heavy sets.

Figure 5 provides accuracy, coverage, and the fraction of vertices removed by the screening for the heavy set reduction. Despite the similar-looking loss values for this reduction rule, it is clear from the other metrics that the models are discovering different things. GCN suggests the least amount of vertices. It also has the highest probability that a suggested vertex can actually be reduced. However, this is at the cost of catching less of the total reducible vertices. GraphSAGE and LR both suggest a larger fraction of the reducible vertices but at the cost of reduced suggestion accuracy and overall screening effect. Note that the models do not have any notion of accuracy or coverage during training, so reducing the loss of training data is the only thing being optimized for during training. To summarize the plots in Figure 5 for LR, it suggests approximately 5% of the graph for the heavy set rule, and among the suggested vertices are approximately 50% of the vertices that actually can be reduced using the heavy set rule.



■ **Figure 5** Accuracy, coverage, and the fraction remaining after the screening for each architecture using the heavy set reduction rule. The values shown here are computed based on the test dataset. Note that the scaling of the y-axes differ.

The final results for all the expensive reduction rules on the test set are given in Table 2. Training all the models took approximately 24 hours on our test machine using PyTorch Geometric [22]. While PyTorch is a powerful framework for quickly developing and training models, several optimizations that could speed up the screening phase in our final program are not utilized. This includes combining the message passing and weighted transformation to reduce the number of times the data needs to pass through the cache hierarchy, loading feature vectors directly into AVX registers, and hard-coding the inner kernels for precisely the dimensions used by the models. To be clear, if the number of features had been higher, PyTorch would undoubtedly perform at a level close to the theoretical limit of the CPU. The optimizations listed above are useful because the number of features is low, and the main bottleneck is the memory bandwidth and latency. For this reason, we only continue with further experiments using one GNN architecture, and we do so using a manual implementation written in C.

Observation 1 Even though the differences are small, LR archives the best training loss and coverage on 5/6 instances compared to GCN and GraphSAGE. Therefore, we proceeded with the LR architecture.

■ **Table 2** Detailed results in percentage on the test data for all reduction rules used in the LEARNANDREDUCE and GNN architectures. Red. refers to the fraction of vertices in the data that can be reduced using the reduction rule. The **best** numbers are shown in bold, where Scr., Cov., Acc., and Loss are compared individually.

Reduction	Red.	GCN				GraphSAGE				LR			
		Scr.	Cov.	Acc.	Loss	Scr.	Cov.	Acc.	Loss	Scr.	Cov.	Acc.	Loss
Critical	6.19	7.03	44.06	38.81	0.45	4.72	31.73	41.63	0.44	6.52	43.99	42.23	0.43
Cut	0.53	0.03	2.89	55.91	0.11	0.00	0.16	24.25	0.10	0.06	8.07	77.80	0.09
Gen. fold	2.45	0.14	2.34	42.17	0.32	0.83	12.68	38.28	0.26	0.98	14.33	36.73	0.25
Heavy set	3.64	2.25	31.39	50.65	0.26	3.77	44.84	43.39	0.26	5.02	51.03	37.13	0.26
Heavy set 3	2.68	0.47	7.88	45.45	0.29	0.51	5.74	30.60	0.34	0.90	9.35	28.00	0.33
Unconfined	7.94	10.15	25.95	25.37	1.45	5.65	17.20	27.07	1.13	30.97	53.36	14.10	0.80

6.4 Learn and Reduce

This section presents experimental results for different configurations of our LEARNANDREDUCE approach. We exclude the vehicle routing instances here since most of them are very hard to reduce by any of our configurations. For the cyclic struction in LEARNANDREDUCE we have the two configurations *Fast* and *Strong* introduced by Gellner et al. [24]. We run the five different screening approaches introduced in Section 4.4 for both of these configurations. In Table 3, we present the average results for all configurations running on the first set of 83 graphs. With the *no gnn red* screening, we can see that these configurations are the fastest but are computing the largest reduced instances. When we use the expensive rule without screening in *never*, we can see the potential gain in reduction size. In the *Fast* configuration, we can further reduce the instances by 13.22% on average when using expensive reduction rules. However, this comes at the cost of more than doubling the preprocessing time on average. All of our *Fast* screening methods can reduce the preprocessing time compared to *never*. The fastest *initial tight* is on average a factor of 1.7 times faster and manages to reduce the instances by an additional 12.59% compared to *no gnn red*. For the *Strong* configurations without screening, we can reduce the instances by 14.94% on average when using the expensive reduction rules. However, the configuration without any expensive rules already takes more time than all of the *Fast* configurations using our screening approach. Therefore, we only focused on the different *Fast* configurations in the following.

In Figure 6, we present two performance profiles comparing the different screening approaches for the *Fast* configuration with additionally running CHILS on the reduced instances afterward. On the left, we have the solution quality achieved using one hour per instance for preprocessing and CHILS. On the right we see the performance profile for the time needed to find the best solution within this time limit. We can see that for all but five instances, all approaches achieve the same solution quality, and for the instances where the quality differs, the differences are minor. When considering the running times however, we can see definite differences. On more than 50% of the instances, not using the expensive reduction rules and having more time for the local search is the best strategy. However, this approach can be multiple orders of magnitude slower in other instances. Not using the screening for expensive rules, i.e. *never* is often more than twice as slow as other configurations. Overall, *initial tight* performed best on most instances regarding running time and is also very close to not using the screening regarding solution quality. There are only four instances where this approach took more than 1.6 times as long as the fastest solver on the respective instance. For all other configurations, this is true for more than 12 instances.

■ **Table 3** Arithmetic mean reduction results. Here, K is the instance reduced by the different configurations, \tilde{K} the instance reduced by *Fast - no gnn red* and G the original graph. We refer to the number of nodes n , and edges m of the different graphs in the index. Furthermore, we give the offset and reduction time. In the column Time exp., we give the time which is used only for expensive reductions and the reduction screening.

Config	GNN	$n_K/n_{\tilde{K}}$	n_K/n_G	m_K/m_G	Offset	Time	Time exp.	# $n_K = 0$
<i>Fast</i>	no gnn red	100.00	5.50	51.13	13 179 456	36.55	0.00	49 / 83
<i>Fast</i>	never	86.78	4.77	50.85	13 270 743	74.74	38.19	52 / 83
<i>Fast</i>	always	87.11	4.79	50.90	13 269 029	65.51	28.96	52 / 83
<i>Fast</i>	initial	87.13	4.79	50.88	13 268 824	58.59	22.04	52 / 83
<i>Fast</i>	initial tight	87.41	4.81	50.91	13 267 958	45.12	8.57	51 / 83
<i>Strong</i>	no gnn red	98.74	5.43	50.81	13 188 267	68.86	0.00	50 / 83
<i>Strong</i>	never	85.06	4.68	50.51	13 280 038	101.56	32.70	53 / 83
<i>Strong</i>	always	85.56	4.71	50.55	13 278 028	107.17	38.31	53 / 83
<i>Strong</i>	initial	85.66	4.71	50.56	13 277 789	88.24	19.38	54 / 83
<i>Strong</i>	initial tight	85.65	4.71	50.58	13 277 974	85.20	16.34	53 / 83

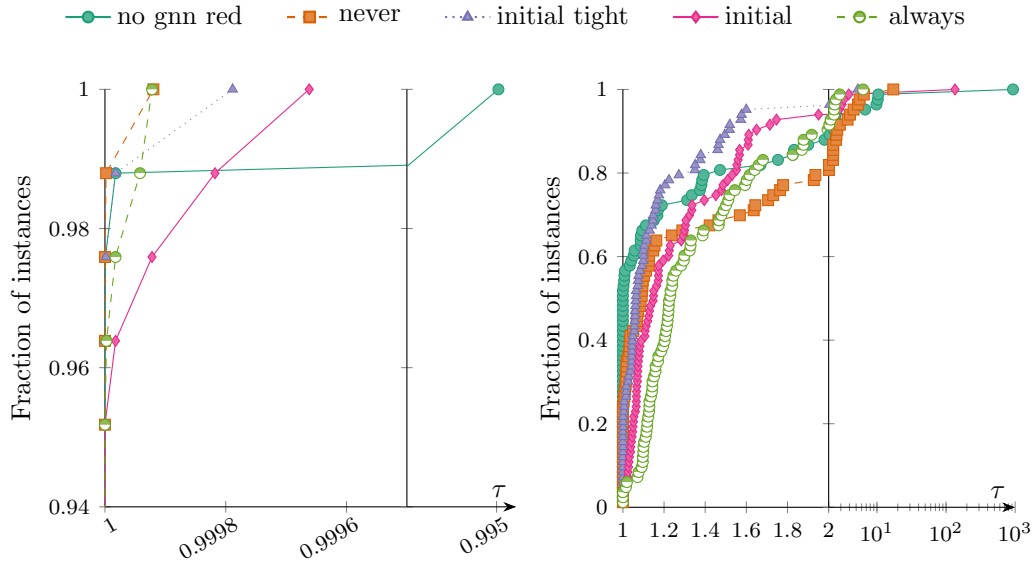
Observation 2 The *Strong* configuration without any expensive rules already takes more time than all of the *Fast* configurations using our screening approach. Therefore, we only focus on the different *Fast* configurations. The *initial tight* performs best overall, especially for more difficult instances. Regarding solution quality, the *initial tight* approach is very close to not using the screening. Therefore, we use the *Fast - initial tight* configuration for our LEARNANDREDUCE routine.

6.5 Parameter Tuning

In this section, we perform experiments to find good choices for the number of concurrent solutions P and the time t spent improving them in the sequential version of CHILS. We choose a subset of our two sets of instances for parameter tuning. We took six graphs from each set. First, two graphs from each graph class of the first set of instances where after *fast early struction* the reduced graph has more than 500 vertices. For the vehicle routing instances, we took three graphs with more than 500 000 vertices and three with less than 500 000 vertices. Note that we did not include any *mesh* or *ssmc* graphs since these are all reduced to less than 500 vertices. The instances chosen for these experiments are marked with a \star in tables 10 and 11.

We begin our experiments with the parameter defining the number of concurrent solutions, $P \in \{8, 16, 32, 48, 64\}$. The second parameter, highly correlating with P , is the time spent per local search run. For this experiment we set $t = t_G = t_C$ and test all $t \in \{0.1, 1, 2.5, 5, 10, 20, 30\}$ seconds. Recall that t_G is the time spent on the original graph and k_C is the time spent on the D-CORE. We present the geometric mean solution weight after one hour for the different configurations of these two parameters in Table 4.

In general, we can see that the best choice for t gets lower as the number of solutions P increase. Comparing the configurations with the most solutions, i.e. $P = 64$, the solution quality is worse than using fewer concurrent local search runs for all t values tested. The best configuration we found is $P = 16$ and $t = 10$ seconds, resulting in a geometric mean weight of 14 132 120. Note that these optimal choices are only for running CHILS sequentially.



■ **Figure 6** Performance profiles for different (*Fast*) LEARNANDREDUCE configurations. After reducing the instance, we run the CHILS heuristic to evaluate the practical impact of the reduction configurations. We present solution quality, including reduction offset (left) and running time including reduction time (right). The vertical line in each plot marks the change from one scale to another.

Observation 3 The best parameter configuration we found experimentally was $P = 16$ and $t = 10$ for running CHILS sequentially with a time limit of one hour per instance.

6.6 State-of-the-Art Comparison

The state-of-the-art comparison in this section is divided into two parts. We start by discussing the results of the first set of instances. Here we compare our algorithms BASELINE and CHILS to state-of-the-art heuristic algorithms HTWIS presented in [29] by Gu et al., the hybrid iterated local search HILS by Nogueira et al. [52] as well as the memetic algorithm $M^2WIS + s$ by Großmann et al. [27]. The second part of this section is dedicated to the other algorithms and results for the vehicle routing instances. For these instances, we compare

■ **Table 4** Geometric mean weight computed by the sequential CHILS after one hour for different configurations for the number of solutions P and time limits for the local search $t = t_G = t_C$. Note that the time t is spent per solution in P , and not divided between them.

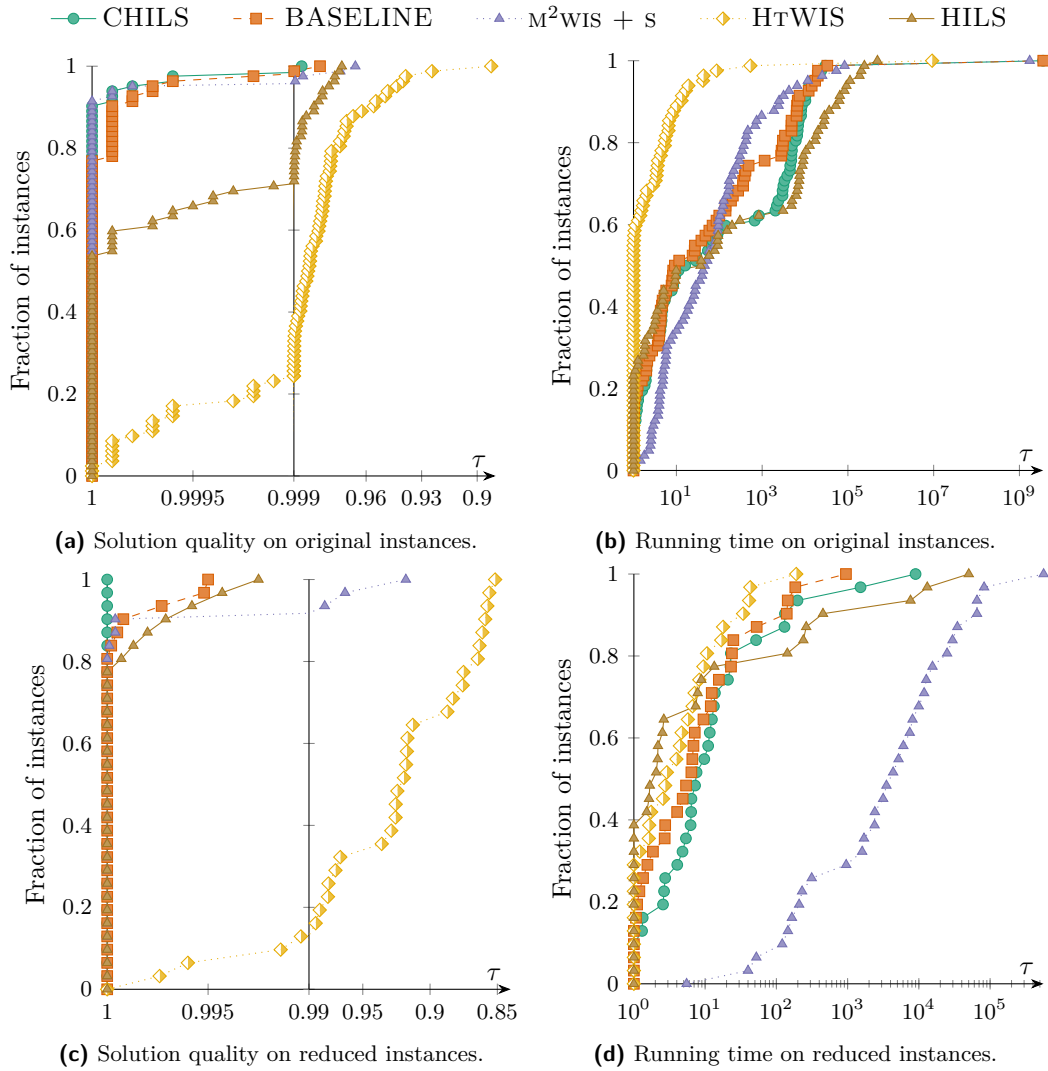
	$P = 8$	$P = 16$	$P = 32$	$P = 64$
$t = 0.1$	14 119 825	14 119 386	14 119 516	14 100 937
$t = 1$	14 124 084	14 126 354	14 127 388	14 117 719
$t = 2.5$	14 127 282	14 128 074	14 130 823	14 118 203
$t = 5$	14 127 913	14 129 545	14 129 347	14 117 284
$t = 10$	14 127 684	14 132 120	14 124 680	14 116 758
$t = 20$	14 130 214	14 125 181	14 119 467	14 110 491
$t = 30$	14 126 896	14 118 547	14 115 472	14 112 364

our heuristics with the results of METAMIS [18]⁴. Additionally, we compare against the new Bregman-Sinkhorn algorithm BSA by Haller et al. [30]. We do not evaluate BSA on the first set of instances as BSA requires clique information that is only available for the vehicle routing instances. Similarly, the vehicle routing instances differ significantly from previously established testing instances. The older state-of-the-art heuristics are not designed or implemented for these instances and perform significantly worse. In splitting the state-of-the-art comparison as described, we evaluate each heuristic in spirit with what they were designed for while demonstrating that BASELINE and CHILS are competitive in both categories.

Table 5 presents results for a subset of graphs from our first set. For this subset we choose the largest four graphs from each graph class. The results on the full set can be found in Table 8 in the Appendix. We can see that both our algorithms BASELINE and CHILS outperform HTWIS and HILS in terms of solution quality on *every* instance. For large instances, such as the *osm* instances, we find these best solutions even faster than any competitor find their best solution within the time limit. When comparing against $M^2WIS + s$, we observe that especially for the *mesh* and *snap* instances, our approaches find slightly worse solutions and need more time. However, $M^2WIS + s$ already uses many of the reductions we incorporated in the LEARNANDREDUCE preprocessing, which we did not use for BASELINE or CHILS. Comparing Table 5 to Table 6 clearly shows the importance of our preprocessing routine. In Table 6, we present the results on the same instances, which have already been reduced with LEARNANDREDUCE. From this it is clear that all evaluated algorithms generally benefit from the preprocessing. On these instances, CHILS finds the best solutions on *all* reduced instances.

In Figure 7, we show performance profiles comparing the different algorithms’ solution quality and running time on the full set of original and reduced instances. Note that most of the solutions on these instances found by $M^2WIS + s$ are optimal [27]. On approximately 60% of the original instances HTWIS finds the solution fastest, see Figures 7b. However, the fast running times come with a decrease in solution quality of up to 10%, as can be seen in Figure 7a. On more than 90% of the instances CHILS finds the best solution while having comparable running times as the other schemes except for HTWIS. The $M^2WIS + s$ algorithm performs very similarly to CHILS on the original instances. However, on the reduced instances, $M^2WIS + s$ has the longest running times; see Figure 7d. Note that the initial reductions used in $M^2WIS + s$ are also included in the LEARNANDREDUCE framework. All other algorithms have similar running times on the reduced instances. From Figure 7c, it follows that all algorithms except for HTWIS find the same solution on almost 80% of the reduced instances. On the other 20% CHILS finds the best solutions which are up to 0.7% better than the HILS solutions and more than 7% better than $M^2WIS + s$. On more than 85% HTWIS computes solutions more than 1% worse than the best solutions found and for approximately 30% of the instances these solutions are even more than 10% worse.

⁴ The code is not publicly available, therefore, we could not rerun the experiments.



■ **Figure 7** Performance profiles for solution quality and running time for original and reduced instances not including the vehicle routing instances. The reduction offset and reduction time are not added for the reduced instances, and fully reduced instances are not included. The vertical line in the plots on the left indicate a change from one scale to another.

Observation 4 All algorithms tested benefit from running the LEARNANDREDUCE preprocessing. CHILS finds the best solution on *all* reduced instances, while performing similar to HILS regarding running time. It is slightly slower than HTWIS, which computes the worst solution quality on these instances. Without preprocessing, the improvement of CHILS over HTWIS and HILS regarding solution quality increases. Here, only M²WIS + s, which already uses reductions, can find better results than CHILS on some graphs.

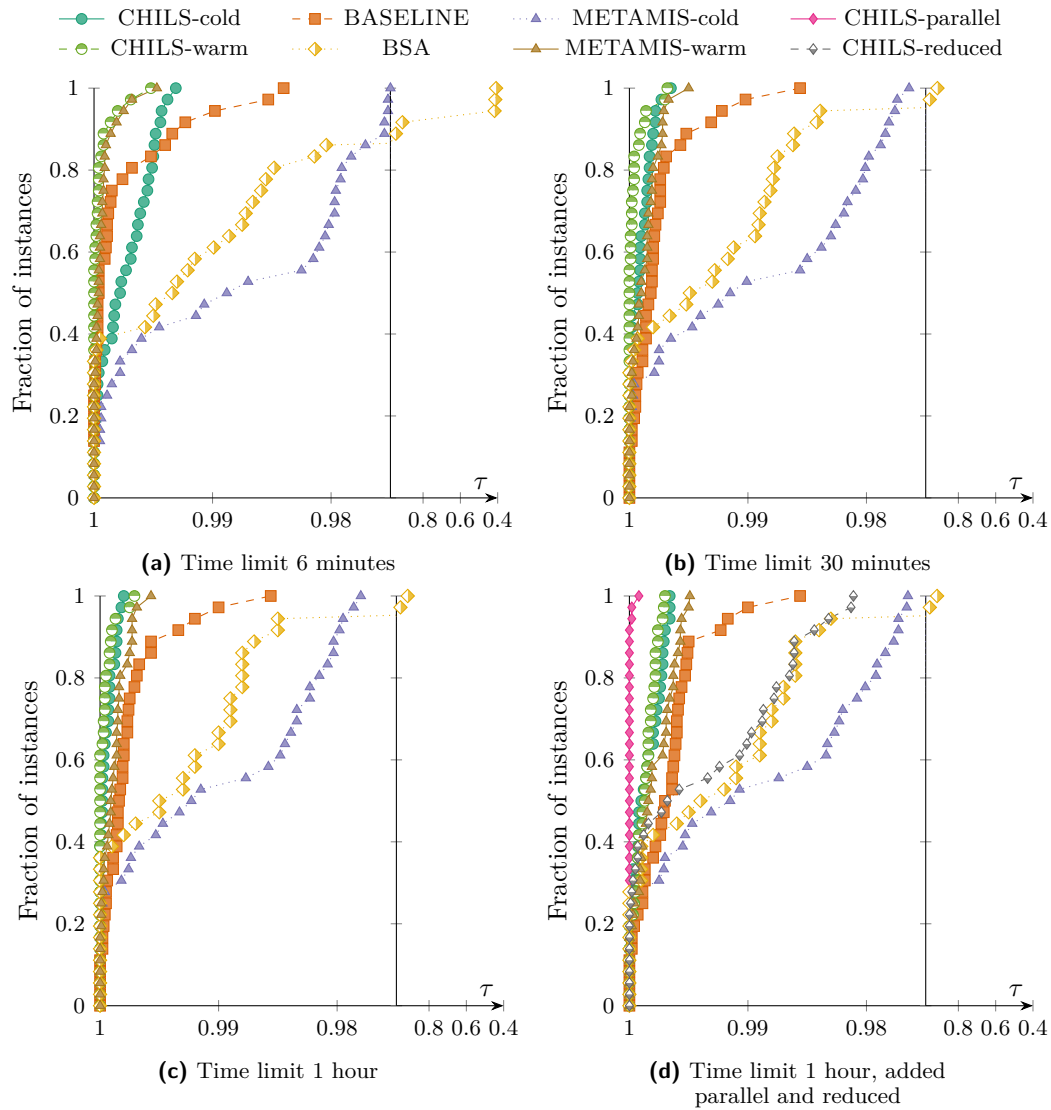
Next, we investigate the results on the second set of instances for the vehicle routing application. Note that the vertex weights for these instances are very large, which leads to only small percentage improvements despite significant differences between the solutions. Here, we only compare against the competitors METAMIS and BSA. In contrast to these

competitors, CHILS and BASELINE are running on the full graph without exploiting the clique information that is also provided. On these instances, most of the solutions found are not optimal, evident by the significantly larger solutions we later find using our parallel CHILS. We add a warm-start configuration for CHILS where we start with the provided initial solution. The METAMIS numbers for cold and warm-starts are taken from [18]. In Figure 8, we present performance profiles to compare the solution quality achieved by the algorithms with different time limits. The first two show the state-of-the-art comparison of solution quality achieved with a 6 and 30 minutes time limit respectively. As expected, the configurations with the warm start perform best with the shortest time limit, see Figure 8a. However, if no initial solution is known, our two variants, BASELINE and CHILS, significantly outperform all competitor configurations. Note that BASELINE is performing better than CHILS on around 80% of the instances here, since the configuration for CHILS is optimized for running with a one-hour time limit, see Section 6.5. Compared to the second profile on the right, we can see that with more time, the CHILS solutions improve most, even surpassing the METAMIS-Warm results in some instances. Within this time limit CHILS-Warm finds the best solutions on almost 60% of the instances. Furthermore, both CHILS configurations compute solutions that are at most 0.3% worse than the best-found solution. On the other hand, on more than 38% of the instances, BSA and METAMIS-Cold find solutions which are more than 1% worse than the best solutions found on the respective instances.

In Figure 8c, we present the state-of-the-art comparison where all algorithms have an hour time limit and run on the original instances. Here, we can see that CHILS with and without the initial solution performs generally the best. The results shown here are very similar to the results computed within the shorter limit of 30 minutes; see Figure 8b.

For the profile in Figure 8d, however, this changes. Here, we added a configuration called CHILS-Parallel, which utilizes the warm start solution and runs in parallel with the configuration of $P = 64$ and $t = 5$ seconds, using 16 parallel threads, i.e. without simultaneous multithreading. Additionally, we used LEARNANDREDUCE and run CHILS on the reduced instances. With this configuration, CHILS-Reduced, we can not compete with the other configurations on most instances since, for these large instances, the reduction rules do not work well; see also Table 11 in the Appendix. It takes considerable time to test even the fast reduction rules on these graphs. However, on *MR-W-FN* or *MW-D-01*, for example, using reduction rules definitely helps to find better solutions; see Table 7. Considering all of our variants, we outperform all other schemes in all but two instances; see Figure 8 and Table 7. Furthermore, our approach is not depending on having good initial solutions as for example METAMIS. Nevertheless, using a warm start solution can improve the performance.

Observation 5 On the vehicle routing instances without initial solutions, even our BASELINE approach outperforms the competitors. The BASELINE approach is especially good with a low time limit. Overall, CHILS outperforms *all* the other heuristics regarding solution quality after 6 minutes, 30 minutes, and 1 hour.



■ **Figure 8** Performance profiles for state-of-the-art comparison on solution quality on the vehicle routing instances with different time limits. In (d), results computed with parallel CHILS and reduction rules are added.

■ **Table 5** Average solution weight ω and time t (in seconds). The **best** solutions among all algorithms are marked in bold. Here, we give the results of the four largest, non-reduced graphs of each class from our first set of instances. The results on all graphs are presented in Table 8 in the Appendix.

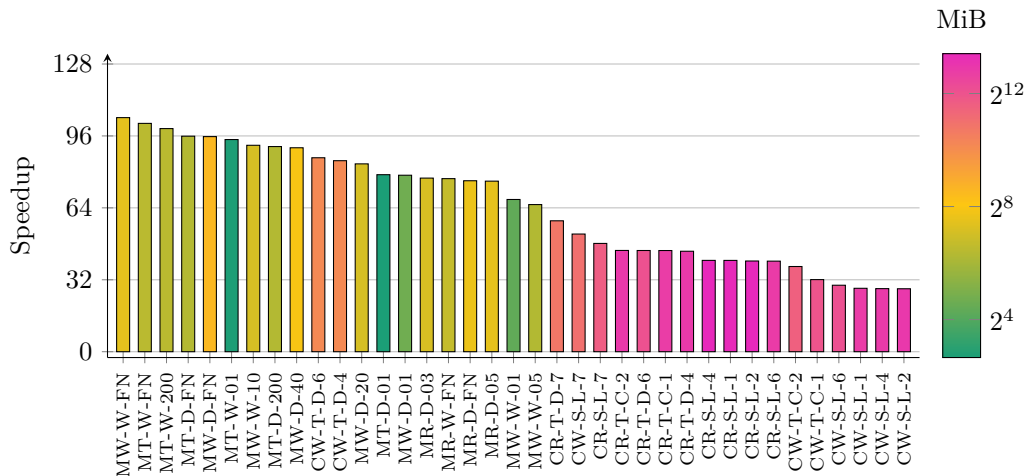
Instance	HrWIS		HILS		M ² WIS + s		BASELINE		CHILS		
	ω	t	ω	t	ω	t	ω	t	ω	t	
fe	body	1 645 650	0.06	1 678 383	3 471.02	1 680 182	2 958.88	1 680 182	1 824.22	1 680 182	165.03
	ocean	6 803 672	0.12	7 081 151	3 384.46	7 248 581	3.38	7 139 076	16.75	7 210 830	2 863.50
	pwt	1 153 600	0.04	1 175 710	3 580.37	1 176 685	3 601.03	1 178 479	49.24	1 178 708	537.13
	rotor	2 591 456	0.31	2 651 471	3 255.65	2 596 217	3 601.17	2 663 757	880.70	2 665 805	3 179.83
mesh	buddha	57 508 556	0.52	56 086 272	3 600.05	57 555 880	4.26	57 554 770	3 380.94	57 555 764	2 571.52
	dragonsub	32 163 872	0.28	31 833 085	3 599.67	32 213 898	1.62	32 212 574	3 409.68	32 213 769	2 857.15
	ecat	36 606 394	0.48	36 122 506	3 600.03	36 650 298	2.60	36 648 982	3 279.35	36 650 039	2 155.87
	turtle	14 247 883	0.14	14 238 437	3 597.64	14 263 005	0.58	14 262 790	2 753.32	14 262 993	1 665.35
osm	d.-of-c.-3	210 461	330.18	227 652	939.72	227 681	1 890.32	227 683	948.94	227 683	258.43
	hawaii-3	134 703	1 423.03	141 041	3 213.04	141 070	2 611.52	141 074	34.12	141 095	160.02
	kentucky-3	97 906	3 077.14	100 510	1 292.90	99 918	3 684.53	100 507	35.39	100 511	160.03
	rhode-i.-3	190 341	255.58	201 753	1 190.44	201 771	1 886.87	201 771	366.29	201 771	15.34
snap	as-skitter	124 141 373	1.17	123 207 288	3 597.32	124 157 729	2 828.19	124 141 585	3 545.45	124 111 689	3 491.32
	roadNet-CA	111 325 524	0.72	108 370 752	3 600.18	111 360 828	4.12	111 355 248	3 496.83	111 358 047	3 579.38
	soc-LiveJ.	283 922 214	9.22	279 386 267	< 0.01	284 036 239	1 737.39	283 951 703	3 599.46	283 924 551	3 562.85
	soc-p.-rel	83 920 370	39.06	82 984 397	3 598.22	81 112 447	3 637.19	83 971 405	3 369.22	83 982 856	3 520.91
ssmc	ca2010	16 792 827	0.55	16 591 401	3 597.70	16 867 553	3 601.26	16 867 987	2 650.77	16 869 278	2 613.13
	fl2010	8 719 272	0.40	8 694 303	3 599.61	8 743 506	183.77	8 742 384	2 941.69	8 743 309	2 832.06
	ga2010	4 639 891	0.21	4 640 168	3 595.16	4 644 417	61.28	4 644 398	579.13	4 644 417	650.90
	il2010	5 963 974	0.39	5 965 735	3 599.95	5 998 539	17.93	5 998 017	2 516.42	5 998 520	3 314.47

■ **Table 6** Average solution weight ω and time t (in seconds). The **best** solutions among all algorithms are marked in bold. Here, we give the results of the graphs from Table 5 reduced with LEARNANDREDUCE. Fully reduced graphs are omitted, reduction offset and reduction time is included in the results. All algorithms are run for one hour on the reduced instances, the LEARNANDREDUCE time was not limited. The results for all graphs are presented in Table 9 in the Appendix. Detailed per instance results for the reduction time and offset are given in Table 10.

Instance		HTWIS		HILS		M ² WIS + s		BASELINE		CHILS	
		ω	t	ω	t	ω	t	ω	t	ω	t
fe	body	1 680 066	0.60	1 680 182	0.61	1 680 182	60.63	1 680 182	0.69	1 680 182	0.68
	pwt	1 169 768	2.21	1 178 273	1 946.51	1 178 735	3 196.24	1 178 735	9.31	1 178 735	9.84
	rotor	2 599 908	5.41	2 653 478	2 764.03	2 617 855	3 606.23	2 664 500	347.16	2 666 222	3 251.99
osm	d.-of-c.-3	217 052	395.81	227 586	734.53	227 622	3 450.79	227 205	350.73	227 656	450.50
	hawaii-3	135 846	1 659.20	140 963	1 068.11	141 076	4 427.01	140 976	1 023.18	141 095	1 785.05
	kentucky-3	99 310	3 421.08	100 475	2 582.95	100 193	5 125.45	100 511	2 167.95	100 511	2 385.14
	rhode-i.-3	197 126	306.81	201 654	184.23	201 767	3 171.02	201 480	167.51	201 771	333.07
snap	as-skitter	124 156 703	3.46	124 157 729	8.63	124 157 729	1 300.24	124 157 700	3.45	124 157 729	33.49
	soc-LiveJ.	284 035 711	23.49	284 036 239	23.65	284 036 239	1 291.80	284 036 239	23.55	284 036 239	23.55
	soc-p.-rel	83 913 297	669.24	83 762 908	4 243.55	81 480 804	4 311.48	83 986 271	4 175.34	83 991 718	3 975.30
ssmc	fl2010	8 742 642	3.62	8 743 506	37.95	8 743 506	1 479.03	8 743 506	3.65	8 743 506	3.65

■ **Table 7** Results for vehicle routing instances by Dong et al. [19]. The results for METAMIS were taken from the paper by Dong et al. [18] since the code is not publicly available. Note that the authors of METAMIS used the best out of four runs, while the results for BASELINE, CHILS, and BSA were only run once. All the results show the best solution found after one hour.

Instance	Cold Start				Warm Start		Reduced	Parallel
	METAMIS	BSA	BASELINE	CHILS	METAMIS	CHILS	CHILS	CHILS
CR-S-L-1	5 588 489	5 639 292	5 694 508	5 698 608	5 692 891	5 701 015	5 610 201	5 718 230
CR-S-L-2	5 691 892	5 729 194	5 785 140	5 798 470	5 784 034	5 799 458	5 715 463	5 813 362
CR-S-L-4	5 681 336	5 725 525	5 781 519	5 791 447	5 777 081	5 792 758	5 698 425	5 806 975
CR-S-L-6	3 859 513	3 900 370	3 936 944	3 938 946	3 936 137	3 946 157	3 890 733	3 952 205
CR-S-L-7	1 989 879	2 006 810	2 017 624	2 021 238	2 019 428	2 022 339	2 006 857	2 025 681
CR-T-C-1	4 654 419	4 717 754	4 742 508	4 744 119	4 743 040	4 750 570	4 702 548	4 760 428
CR-T-C-2	4 874 346	4 934 488	4 969 512	4 975 069	4 968 952	4 976 613	4 918 257	4 987 562
CR-T-D-4	4 817 281	4 875 268	4 912 984	4 919 079	4 911 646	4 922 752	4 864 858	4 932 826
CR-T-D-6	2 970 011	3 009 020	3 024 044	3 027 211	3 024 523	3 029 782	2 999 231	3 033 189
CR-T-D-7	1 440 281	1 453 990	1 460 328	1 461 099	1 460 240	1 460 584	1 451 070	1 462 239
CW-S-L-1	1 634 950	1 645 459	1 660 063	1 660 472	1 660 815	1 662 580	1 646 548	1 663 763
CW-S-L-2	1 708 820	1 713 535	1 737 052	1 738 307	1 738 128	1 739 670	1 723 914	1 743 532
CW-S-L-4	1 725 591	1 730 641	1 751 204	1 754 409	1 753 803	1 756 602	1 735 633	1 759 452
CW-S-L-6	1 158 925	1 162 552	1 175 335	1 177 272	1 177 156	1 176 354	1 166 774	1 178 467
CW-S-L-7	587 288	588 279	594 312	594 598	593 891	593 807	590 834	594 757
CW-T-C-1	1 317 775	1 325 862	1 336 232	1 338 085	1 338 064	1 340 085	1 323 170	1 341 888
CW-T-C-2	931 802	935 238	944 902	946 217	945 886	945 913	935 907	947 644
CW-T-D-4	457 185	459 575	460 955	460 734	461 056	461 108	459 543	461 475
CW-T-D-6	457 790	459 238	461 088	461 354	461 312	461 101	460 227	461 709
MR-D-03	1 754 110 286	1 757 141 345	1 752 894 190	1 758 762 733	1 757 227 519	1 758 429 721	1 758 775 738	1 759 255 435
MR-D-05	1 786 342 921	1 788 812 740	1 781 868 583	1 789 601 100	1 787 849 777	1 789 537 256	1 789 944 187	1 790 776 639
MR-D-FN	1 797 573 192	1 801 983 754	1 794 240 970	1 801 499 264	1 799 452 160	1 800 375 890	1 801 727 328	1 802 925 854
MR-W-FN	5 358 386 615	5 386 842 780	5 385 799 979	5 385 799 979	5 386 842 781	5 386 842 781	5 386 842 781	5 386 842 781
MT-D-01	238 166 485	238 166 485	238 166 485	238 166 485	238 166 485	238 166 485	238 166 485	238 166 485
MT-D-200	287 048 909	287 155 108	287 042 596	287 086 442	287 048 081	287 042 596	287 086 442	287 086 442
MT-D-FN	290 866 943	290 866 943	290 866 943	290 866 943	290 771 450	290 771 450	290 866 943	290 866 943
MT-W-01	312 121 568	312 121 568	312 121 568	312 121 568	312 121 568	312 121 568	312 121 568	312 121 568
MT-W-200	383 961 323	384 056 011	383 974 084	384 052 157	383 985 408	384 052 017	384 052 157	384 056 012
MT-W-FN	390 854 593	390 869 890	390 869 891	390 869 891	390 869 891	390 869 891	390 869 891	390 869 891
MW-D-01	476 334 711	476 298 607	475 180 516	476 328 138	475 987 082	476 120 423	476 440 656	476 360 408
MW-D-20	525 124 575	526 857 183	523 423 307	526 883 302	525 486 034	526 333 489	526 648 329	527 498 481
MW-D-40	536 520 199	539 036 121	533 671 730	538 302 190	536 915 155	537 485 389	538 409 586	538 596 069
MW-D-FN	541 918 916	545 554 192	541 193 604	544 451 893	543 857 187	544 205 239	544 246 489	545 711 017
MW-W-01	1 270 305 952	1 270 305 952	1 270 305 952	1 270 235 200	1 269 344 846	1 269 344 846	1 270 305 952	1 270 305 952
MW-W-05	1 328 958 047	1 326 236 043	1 327 478 708	1 328 043 785	1 328 958 047	1 328 958 047	1 328 043 785	1 328 958 047
MW-W-10	1 342 899 725	1 280 286 209	1 340 268 013	1 342 808 634	1 342 915 691	1 342 915 691	1 342 809 954	1 342 915 691
MW-W-FN	1 350 818 543	1 235 306 258	1 331 333 002	1 350 818 543	1 350 818 543	1 350 818 543	1 350 818 543	1 350 818 543



■ **Figure 9** Bar chart showing the speedup on each instance using 128 threads compared to the sequential CHILS. The colors indicate the amount of allocated memory for each instance. The total amount of L3 cache for this machine is 256 MiB, and smaller instances fit entirely in the cache.

6.7 Parallel Scalability

For the parallel results shown in Figure 8d, we used the same machine as the other heuristics to ensure fairness between each program with regard to solution quality. To gain more detailed insight into the parallel scalability of our approach, we utilize a larger machine with an AMD EPYC 9754 128-core processor for our scalability experiments. Furthermore, CHILS as defined in Section 5 relies on wall time to alternate between local search on the full graph and the D-CORE. This introduces variance between runs and makes it difficult to conduct scalability experiments. Therefore, we change the implementation for this section to perform a fixed number of local search iterations instead, where one iteration refers to the while loop starting on Line 2 in Algorithm 5. We also set a fixed number of CHILS iterations, referring to the while loop starting on Line 2 in Algorithm 6. By removing the wall-clock measures and using the same random seed, we ensure that the parallel and sequential versions perform the exact same computations and reach the same solution in the end.

The configuration we use for these experiments consists of 1,000 local search iterations, 10 CHILS iterations, and $P = 128$. Depending on the instance, this ratio of local search on the full graph and D-CORE is reasonably close to the wall-clock version with $t_G = t_C = 10$. Each run was repeated five times, and the best measurement is used. We use the best measurement because, in this configuration, there is no randomness between runs. Any difference we observe in execution time is solely due to factors outside our control, such as fluctuations in clock speed and other programs running on the machine. As such, the best measure is the closest to the true execution time.

The speedup numbers for each instance are shown in Figure 9. The best scaling instance reaches a speedup of 104, while the worst is still 28 times faster than the sequential program. Figure 9 also shows the amount of memory allocated for each instance. This includes the graph, which we store using the compressed sparse row format, and additional data structures required by the heuristic. All memory allocations are done up front before starting the heuristic, and the appropriate thread initializes any thread-local data. The CPU we use has a combined L3 cache of 256 MiB. There is a clear drop in speedup around the point when the data no longer fits in the cache. This indicates that the memory bandwidth is the main

bottleneck for larger instances. In terms of load balancing, there could be variations in how much work it takes to perform 1,000 local search iterations for each solution. This is because each solution has a different random seed and m_q parameter. Note that this is not an issue for the version presented in Section 5, since that version uses wall time instead of local search iterations. Table 10 in the Appendix gives detailed execution time, speedup, and the amount of memory used for each instance.

7 Conclusion and Future Work

We have introduced LEARNANDREDUCE, a preprocessing algorithm for the MWIS problem that combines Graph Neural Networks (GNNs) with a large collection of reduction rules to reduce further and faster than previously possible. In addition to using known data reduction rules, we also introduce seven new reduction rules. The GNNs are trained to predict where we can apply costly reduction rules to speed up the reduction process. Combined, this strikes a good balance between speed and quality at the preprocessing stage. In addition to exact preprocessing, we also introduce a new heuristic called CHILS (Concurrent Hybrid Iterated Local Search) that expands on the HILS heuristic. This new heuristic outperforms all known heuristics across a wide range of test instances in a sequential environment. As an added benefit, CHILS can also leverage the power offered by multicore processors. Letting CHILS use all 16 cores available on our test machine significantly improves the solution quality on the hardest instances in our dataset.

The vehicle routing instances by Dong et al. [19] offer a significant challenge for practical MWIS algorithms. Our result marks the third iteration of improvements to this dataset, after METAMIS [18] and BSA [30], and yet, we are still far away from optimal solutions on these instances. This is evident by the significant uplift in solution quality by running CHILS in parallel. Using another 128-core machine for scalability experiments, we show that CHILS reaches speedups up to 104 for the vehicle routing instances.

There are several directions for future research, including finding efficient data reductions that work on these hard instances or using the clique information in the CHILS heuristic. If the use of clique information leads to improvements, then a natural continuation would be to compute clique covers for other hard instances.

We have also introduced a supervised learning dataset for MWIS reductions. The models we use in LEARNANDREDUCE are trained on this dataset. In this work, we only considered the most common GNN architectures and only the application of reduction rule screening. Besides trying more complicated architectures, there are other directions for further work starting from this dataset. One promising direction is to use GNN models to reduce the graph directly. Even though this would no longer be exact preprocessing it could lead to a powerful heuristic.

CHILS is based on the proposed metaheuristic CONCURRENT DIFFERENCE-CORE HEURISTIC. This metaheuristic could lead to improvements in heuristics for other problems as well. As a metaheuristic, it only requires that solutions can be compared to find the DIFFERENCE-CORE; otherwise, any heuristic method can be used internally. Examples of problems to try include VERTEX COVER, DOMINATING SET, GRAPH COLORING, and CONNECTIVITY AUGMENTATION. As an added benefit, the CONCURRENT DIFFERENCE-CORE HEURISTIC is trivially parallelizable, which could enable improvements in the parallel setting too.

References

- 1 KaMIS Source Code. URL: <https://github.com/KarlsruheMIS/KaMIS>.
- 2 OpenStreetMap. URL: <https://www.openstreetmap.org>.
- 3 SuiteSparse Matrix Collection. URL: <https://sparse.tamu.edu>.
- 4 Faisal N. Abu-Khzam, Sebastian Lamm, Matthias Mnich, Alexander Noe, Christian Schulz, and Darren Strash. Recent advances in practical data reduction. In Hannah Bast, Claudius Korzen, Ulrich Meyer, and Manuel Penschuck, editors, *Algorithms for Big Data: DFG Priority Program 1736*, pages 97–133. Springer Nature Switzerland, Cham, 2022. doi:10.1007/978-3-031-21534-6_6.
- 5 T. Akiba and Y. Iwata. Branch-and-reduce exponential/FPT algorithms in practice: A case study of vertex cover. *Theoretical Computer Science*, 609, Part 1:211–225, 2016. doi:10.1016/j.tcs.2015.09.023.
- 6 Gabriela Alexe, Peter L Hammer, Vadim V Lozin, and Dominique de Werra. Structon revisited. *Discrete applied mathematics*, 132(1-3):27–46, 2003. doi:10.1016/S0166-218X(03)00388-3.
- 7 Diogo V. Andrade, Mauricio G.C. Resende, and Renato F. Werneck. Fast local search for the maximum independent set problem. *Journal of Heuristics*, 18(4):525–547, 2012. doi:10.1007/s10732-012-9196-4.
- 8 Luitpold Babel. A fast algorithm for the maximum weight clique problem. *Computing*, 52(1):31–38, 1994. doi:10.1007/BF02243394.
- 9 Egon Balas and Chang Sung Yu. Finding a maximum clique in an arbitrary graph. *SIAM Journal on Computing*, 15(4):1054–1068, 1986. doi:10.1137/0215075.
- 10 Max Bannach and Sebastian Berndt. Pace solver description: The pace 2023 parameterized algorithms and computational experiments challenge: Twinwidth. In *18th International Symposium on Parameterized and Exact Computation (IPEC 2023)*. Schloss-Dagstuhl-Leibniz Zentrum für Informatik, 2023.
- 11 Lukas Barth, Benjamin Niedermann, Martin Nöllenburg, and Darren Strash. Temporal map labeling: A new unified framework with experiments. In *Proceedings of the 24th ACM SIGSPATIAL International Conference on Advances in Geographic Information Systems*, GIS '16, pages 23:1–23:10. ACM, 2016. doi:10.1145/2996913.2996957.
- 12 Sergiy Butenko. *Maximum independent set and related problems, with applications*. University of Florida, 2003.
- 13 Sergiy Butenko and Svyatoslav Trukhanov. Using critical sets to solve the maximum independent set problem. *Operations Research Letters*, 35(4):519–524, 2007. doi:10.1016/j.orl.2006.07.004.
- 14 Shaowei Cai, Wenying Hou, Jinkun Lin, and Yuanjie Li. Improving local search for minimum weight vertex cover by dynamic strategies. In *Proceedings of the Twenty-Seventh International Joint Conference on Artificial Intelligence (IJCAI 2018)*, pages 1412–1418, 2018. doi:10.24963/ijcai.2018/196.
- 15 Shaowei Cai, Kaile Su, and Abdul Sattar. Local search with edge weighting and configuration checking heuristics for minimum vertex cover. *Artificial Intelligence*, 175(9-10):1672–1696, 2011. doi:10.1016/j.artint.2011.03.003.
- 16 Timothy A Davis and Yifan Hu. The university of florida sparse matrix collection. *ACM Transactions on Mathematical Software (TOMS)*, 38(1):1–25, 2011.
- 17 Elizabeth D Dolan and Jorge J Moré. Benchmarking optimization software with performance profiles. *Mathematical programming*, 91(2):201–213, 2002. doi:10.1007/s101070100263.
- 18 Yuanyuan Dong, Andrew V. Goldberg, Alexander Noe, Nikos Parotsidis, Mauricio G. C. Resende, and Quico Spaen. A metaheuristic algorithm for large maximum weight independent set problems. *CoRR*, abs/2203.15805, 2022. URL: <https://doi.org/10.48550/arXiv.2203.15805>, arXiv:2203.15805, doi:10.48550/ARXIV.2203.15805.
- 19 Yuanyuan Dong, Andrew V Goldberg, Alexander Noe, Nikos Parotsidis, Mauricio GC Resende, and Quico Spaen. New instances for maximum weight independent set from a vehicle routing application. In *Operations Research Forum*, volume 2, pages 1–6. Springer, 2021.

- 20 Ch Ebenegger, PL Hammer, and D De Werra. Pseudo-boolean functions and stability of graphs. In *North-Holland mathematics studies*, volume 95, pages 83–97. Elsevier, 1984. doi:10.1016/S0304-0208(08)72955-4.
- 21 Zhiwen Fang, Chu-Min Li, and Ke Xu. An exact algorithm based on maxsat reasoning for the maximum weight clique problem. *Journal of Artificial Intelligence Research*, 55:799–833, 2016.
- 22 Matthias Fey and Jan E. Lenssen. Fast graph representation learning with PyTorch Geometric. In *ICLR Workshop on Representation Learning on Graphs and Manifolds*, 2019.
- 23 Aleksander Figiel, Vincent Froese, André Nichterlein, and Rolf Niedermeier. There and back again: On applying data reduction rules by undoing others. In Shiri Chechik, Gonzalo Navarro, Eva Rotenberg, and Grzegorz Herman, editors, *30th Annual European Symposium on Algorithms, ESA 2022, September 5-9, 2022, Berlin/Potsdam, Germany*, volume 244 of *LIPICs*, pages 53:1–53:15. Schloss Dagstuhl - Leibniz-Zentrum für Informatik, 2022. doi:10.4230/LIPICs.ESA.2022.53.
- 24 Alexander Gellner, Sebastian Lamm, Christian Schulz, Darren Strash, and Bogdán Zaválnij. Boosting data reduction for the maximum weight independent set problem using increasing transformations. In *2021 Proceedings of the Workshop on Algorithm Engineering and Experiments (ALENEX)*, pages 128–142. SIAM, 2021.
- 25 Kazushige Goto and Robert A van de Geijn. Anatomy of high-performance matrix multiplication. *ACM Transactions on Mathematical Software (TOMS)*, 34(3):1–25, 2008.
- 26 Ernestine Großmann, Tobias Heuer, Christian Schulz, and Darren Strash. The PACE 2022 parameterized algorithms and computational experiments challenge: directed feedback vertex set. In *17th International Symposium on Parameterized and Exact Computation (IPEC 2022)*. Schloss-Dagstuhl-Leibniz Zentrum für Informatik, 2022.
- 27 Ernestine Großmann, Sebastian Lamm, Christian Schulz, and Darren Strash. Finding near-optimal weight independent sets at scale. In Sara Silva and Luís Paquete, editors, *Proceedings of the Genetic and Evolutionary Computation Conference, GECCO 2023, Lisbon, Portugal, July 15-19, 2023*, pages 293–302. ACM, 2023. doi:10.1145/3583131.3590353.
- 28 Ernestine Großmann, Kenneth Langedal, and Christian Schulz. A comprehensive survey of data reduction rules for the maximum weighted independent set problem, 2024. URL: <https://arxiv.org/abs/2412.09303>, arXiv:2412.09303.
- 29 Jiewei Gu, Weiguo Zheng, Yuzheng Cai, and Peng Peng. Towards computing a near-maximum weighted independent set on massive graphs. In *Proceedings of the 27th ACM SIGKDD Conference on Knowledge Discovery & Data Mining*, pages 467–477, 2021.
- 30 Stefan Haller and Bogdan Savchynskyy. A bregman-sinkhorn algorithm for the maximum weight independent set problem. *arXiv preprint arXiv:2408.02086*, 2024.
- 31 Stefan Haller and Bogdan Savchynskyy. Personal communication, 2024.
- 32 Will Hamilton, Zhitao Ying, and Jure Leskovec. Inductive representation learning on large graphs. *Advances in neural information processing systems*, 30, 2017.
- 33 Stephan Held, William Cook, and Edward C Sewell. Maximum-weight stable sets and safe lower bounds for graph coloring. *Mathematical Programming Computation*, 4(4):363–381, 2012.
- 34 Demian Hesse, Sebastian Lamm, and Christian Schorr. Targeted branching for the maximum independent set problem. *arXiv preprint arXiv:2102.01540*, 2021.
- 35 Demian Hesse, Sebastian Lamm, Christian Schulz, and Darren Strash. WeGotYouCovered: The winning solver from the PACE 2019 challenge, vertex cover track. In *2020 Proceedings of the SIAM Workshop on Combinatorial Scientific Computing*, pages 1–11. SIAM, 2020. doi:10.1137/1.9781611976229.1.
- 36 Hua Jiang, Chu-Min Li, and Filip Manyá. An exact algorithm for the maximum weight clique problem in large graphs. In *AAAI*, pages 830–838, 2017.
- 37 Richard M Karp. *Reducibility among combinatorial problems*. Springer, 2010.
- 38 Leon Kellerhals, Tomohiro Koana, André Nichterlein, and Philipp Zschoche. The PACE 2021 parameterized algorithms and computational experiments challenge: Cluster editing.

- In *16th International Symposium on Parameterized and Exact Computation (IPEC 2021)*. Schloss-Dagstuhl-Leibniz Zentrum für Informatik, 2021.
- 39 Diederik P Kingma and Jimmy Ba. Adam: A method for stochastic optimization. *arXiv preprint arXiv:1412.6980*, 2014.
 - 40 Thomas N Kipf and Max Welling. Semi-supervised classification with graph convolutional networks. *arXiv preprint arXiv:1609.02907*, 2016.
 - 41 Danai Koutra, Henning Meyerhenke, Ilya Safro, and Fabian Brandt-Tumescheit. Scalable graph mining and learning (dagstuhl seminar 23491). 2024.
 - 42 Sebastian Lamm, Peter Sanders, and Christian Schulz. Graph partitioning for independent sets. In *International Symposium on Experimental Algorithms*, pages 68–81. Springer, 2015.
 - 43 Sebastian Lamm, Peter Sanders, Christian Schulz, Darren Strash, and Renato F. Werneck. Finding near-optimal independent sets at scale. *Journal of Heuristics*, 23(4):207–229, 2017. doi:10.1007/s10732-017-9337-x.
 - 44 Sebastian Lamm, Christian Schulz, Darren Strash, Robert Williger, and Huashuo Zhang. Exactly solving the maximum weight independent set problem on large real-world graphs. In *2019 Proceedings of the Twenty-First Workshop on Algorithm Engineering and Experiments (ALENEX)*, pages 144–158. SIAM, 2019. doi:10.1137/1.9781611975499.12.
 - 45 Kenneth Langedal, Demian Hesse, and Peter Sanders. Targeted branching for the maximum independent set problem using graph neural networks. In *22nd International Symposium on Experimental Algorithms (SEA 2024)*. Schloss Dagstuhl–Leibniz-Zentrum für Informatik, 2024.
 - 46 Kenneth Langedal, Johannes Langguth, Fredrik Manne, and Daniel Thilo Schroeder. Efficient minimum weight vertex cover heuristics using graph neural networks. In *20th International Symposium on Experimental Algorithms (SEA 2022)*. Schloss Dagstuhl-Leibniz-Zentrum für Informatik, 2022.
 - 47 Juho Lauri, Sourav Dutta, Marco Grassia, and Deepak Ajwani. Learning fine-grained search space pruning and heuristics for combinatorial optimization. *Journal of Heuristics*, 29(2):313–347, 2023.
 - 48 Jure Leskovec and Andrej Krevl. SNAP Datasets: Stanford large network dataset collection. URL <http://snap.stanford.edu/data>, June 2014.
 - 49 Chu-Min Li, Hua Jiang, and Felip Manyà. On minimization of the number of branches in branch-and-bound algorithms for the maximum clique problem. *Computers & Operations Research*, 84:1–15, 2017. doi:10.1016/j.cor.2017.02.017.
 - 50 Ruizhi Li, Shuli Hu, Shaowei Cai, Jian Gao, Yiyuan Wang, and Minghao Yin. Numwvc: A novel local search for minimum weighted vertex cover problem. *J. Oper. Res. Soc.*, 71(9):1498–1509, 2020. doi:10.1080/01605682.2019.1621218.
 - 51 Yuanjie Li, Shaowei Cai, and Wenying Hou. An efficient local search algorithm for minimum weighted vertex cover on massive graphs. In Yuhui Shi, Kay Chen Tan, Mengjie Zhang, Ke Tang, Xiaodong Li, Qingfu Zhang, Ying Tan, Martin Middendorf, and Yaochu Jin, editors, *Simulated Evolution and Learning - 11th International Conference, SEAL 2017, Shenzhen, China, November 10-13, 2017, Proceedings*, volume 10593 of *Lecture Notes in Computer Science*, pages 145–157. Springer, 2017. doi:10.1007/978-3-319-68759-9_13.
 - 52 Bruno Nogueira, Rian G. S. Pinheiro, and Anand Subramanian. A hybrid iterated local search heuristic for the maximum weight independent set problem. *Optimization Letters*, 12(3):567–583, 2018. doi:10.1007/s11590-017-1128-7.
 - 53 Patric RJ Östergård. A fast algorithm for the maximum clique problem. *Discrete Applied Mathematics*, 120(1-3):197–207, 2002. doi:10.1016/S0166-218X(01)00290-6.
 - 54 Rick Plachetta and Alexander van der Grinten. Sat-and-reduce for vertex cover: Accelerating branch-and-reduce by sat solving. In *2021 Proceedings of the Workshop on Algorithm Engineering and Experiments (ALENEX)*, pages 169–180. SIAM, 2021.
 - 55 Steffen Rebennack, Marcus Oswald, Dirk Oliver Theis, Hanna Seitz, Gerhard Reinelt, and Panos M Pardalos. A branch and cut solver for the maximum stable set problem. *Journal of combinatorial optimization*, 21(4):434–457, 2011. doi:10.1007/s10878-009-9264-3.

- 56 Pedro V Sander, Diego Nehab, Eden Chlamtac, and Hugues Hoppe. Efficient traversal of mesh edges using adjacency primitives. *ACM Transactions on Graphics (TOG)*, 27(5):1–9, 2008. doi:10.1145/1409060.1409097.
- 57 Sándor Szabó and Bogdán Zavalnij. Combining algorithms for vertex cover and clique search. In *Proceedings of the 22nd International Multiconference INFORMATION SOCIETY – IS 2019, Volume I: Middle-European Conference on Applied Theoretical Computer Science*, pages 71–74, 2019.
- 58 Chris Walshaw. Graph partitioning archive. URL <https://chriswalshaw.co.uk/partition/>, 2000.
- 59 Luzhi Wang, Chu-Min Li, Junping Zhou, Bo Jin, and Minghao Yin. An exact algorithm for minimum weight vertex cover problem in large graphs. *Computing Research Repository (CoRR)*, abs/1903.05948, 2019. doi:10.48550/ARXIV.1903.05948.
- 60 Jeffrey S Warren and Illya V Hicks. Combinatorial branch-and-bound for the maximum weight independent set problem. *Relatório Técnico, Texas A&M University, Citeseer*, 9:17, 2006.
- 61 Deepak Warriar. *A branch, price, and cut approach to solving the maximum weighted independent set problem*. PhD thesis, Texas A&M University, 2007. doi:1969.1/5814.
- 62 Deepak Warriar, Wilbert E Wilhelm, Jeffrey S Warren, and Illya V Hicks. A branch-and-price approach for the maximum weight independent set problem. *Networks: An International Journal*, 46(4):198–209, 2005. doi:10.1002/net.20088.
- 63 Zonghan Wu, Shirui Pan, Fengwen Chen, Guodong Long, Chengqi Zhang, and S Yu Philip. A comprehensive survey on graph neural networks. *IEEE transactions on neural networks and learning systems*, 32(1):4–24, 2020.
- 64 Mingyu Xiao, Sen Huang, and Xiaoyu Chen. Maximum weighted independent set: Effective reductions and fast algorithms on sparse graphs. *Algorithmica*, 86(5):1293–1334, 2024. URL: <https://doi.org/10.1007/s00453-023-01197-x>, doi:10.1007/S00453-023-01197-X.
- 65 Mingyu Xiao, Sen Huang, Yi Zhou, and Bolin Ding. Efficient reductions and a fast algorithm of maximum weighted independent set. In *Proceedings of the Web Conference 2021*, pages 3930–3940, 2021.
- 66 Mingyu Xiao and Hiroshi Nagamochi. Confining sets and avoiding bottleneck cases: A simple maximum independent set algorithm in degree-3 graphs. *Theor. Comput. Sci.*, 469:92–104, 2013. URL: <https://doi.org/10.1016/j.tcs.2012.09.022>, doi:10.1016/J.TCS.2012.09.022.
- 67 Hong Xu, TK Satish Kumar, and Sven Koenig. A new solver for the minimum weighted vertex cover problem. In *International Conference on AI and OR Techniques in Constraint Programming for Combinatorial Optimization Problems*, pages 392–405. Springer, 2016. doi:10.1007/978-3-319-33954-2_28.
- 68 Weiguo Zheng, Jiewei Gu, Peng Peng, and Jeffrey Xu Yu. Efficient weighted independent set computation over large graphs. In *IEEE Intl. Conf. on Data Engineering (ICDE)*, pages 1970–1973, 2020. doi:10.1109/ICDE48307.2020.00216.

A State-of-the-Art Results

■ **Table 8** Average solution weight ω and time t (in seconds) required to compute it for the *non reduced* instances from set one. The **best** solutions among all algorithms are marked bold.

Instance		HTWIS		HILS		M ² WIS + s		BASELINE		CHILS	
		ω	t	ω	t	ω	t	ω	t	ω	t
fe	body	1 645 650	0.06	1 678 383	3 471.02	1 680 182	2 958.88	1 680 182	1 824.22	1 680 182	165.03
	ocean	6 803 672	0.12	7 081 151	3 384.46	7 248 581	3.38	7 139 076	16.75	7 210 830	2 863.50
	pwt	1 153 600	0.04	1 175 710	3 580.37	1 176 685	3 601.03	1 178 479	49.24	1 178 708	537.13
	rotor	2 591 456	0.31	2 651 471	3 255.65	2 596 217	3 601.17	2 663 757	880.70	2 665 805	3 179.83
	sphere	608 401	0.02	617 139	3 166.86	617 816	1.95	617 738	6.05	617 816	125.55
mesh	blob	854 484	< 0.01	855 004	252.71	855 547	0.04	855 544	0.26	855 547	45.37
	buddha	57 508 556	0.52	56 086 272	3 600.05	57 555 880	4.26	57 554 770	3 380.94	57 555 764	2 571.52
	bunny	3 682 356	0.04	3 681 110	3 415.81	3 686 960	0.14	3 686 896	15.13	3 686 960	167.07
	dragonsub	32 163 872	0.28	31 833 085	3 599.67	32 213 898	1.62	32 212 574	3 409.68	32 213 769	2 857.15
	dragon	7 950 526	0.07	7 946 347	3 485.87	7 956 530	0.27	7 956 496	32.35	7 956 526	160.64
	ecat	36 606 394	0.48	36 122 506	3 600.03	36 650 298	2.60	36 648 982	3 279.35	36 650 039	2 155.87
	fan disk	462 765	< 0.01	463 049	3 212.81	463 288	0.02	463 280	2.37	463 288	21.82
	feline	2 204 947	0.03	2 204 823	3 055.87	2 207 219	0.10	2 207 213	1.60	2 207 219	105.20
	gameguy	2 324 088	0.02	2 323 182	3 553.14	2 325 878	0.06	2 325 802	5.25	2 325 878	42.04
	gargoyle	1 058 656	< 0.01	1 059 102	2 337.95	1 059 559	0.05	1 059 559	1.35	1 059 559	1.35
	turtle	14 247 883	0.14	14 238 437	3 597.64	14 263 005	0.58	14 262 790	2 753.32	14 262 993	1 665.35
	osm	alabama-2	172 797	0.01	174 309	0.11	174 309	0.03	174 309	0.10	174 309
alabama-3		182 667	0.52	185 744	0.30	185 744	28.95	185 744	14.44	185 744	16.45
california-2		45 377	< 0.01	47 153	< 0.01	47 153	0.03	47 153	< 0.01	47 153	< 0.01
california-3		48 356	0.04	49 365	0.08	49 365	19.04	49 365	0.05	49 365	0.05
canada-3		84 503	0.02	86 018	0.01	86 018	2.07	86 018	< 0.01	86 018	< 0.01
colorado-3		54 435	< 0.01	54 741	0.03	54 741	0.07	54 741	0.02	54 741	0.02
d.-of-c.-1		193 364	0.02	196 475	1.05	196 475	1.06	196 475	0.07	196 475	0.04
d.-of-c.-2		198 327	2.40	209 132	476.45	209 132	1 643.20	209 132	64.28	209 132	160.18

Continued on next page

Table 8 – *Continued from previous page*

Instance	HTWIS		HILS		M ² WIS + S		BASELINE		CHILS	
	ω	t	ω	t	ω	t	ω	t	ω	t
d.-of-c.-3	210 461	330.18	227 652	939.72	227 681	1 890.32	227 683	948.94	227 683	258.43
florida-3	234 218	0.20	237 333	1.94	237 333	6.91	237 333	1.14	237 333	1.13
georgia-3	218 573	0.13	222 652	0.04	222 652	5.99	222 652	0.15	222 652	0.15
greenland-2	10 179	0.06	10 718	0.13	10 718	0.68	10 718	0.24	10 718	0.23
greenland-3	12 505	34.22	14 012	3 131.30	14 011	1 360.74	14 012	180.88	14 012	161.13
hawaii-2	123 173	0.19	125 284	0.12	125 284	0.31	125 284	1.03	125 284	1.04
hawaii-3	134 703	1 423.03	141 041	3 213.04	141 070	2 611.52	141 074	34.12	141 095	160.02
idaho-3	75 527	52.15	77 145	115.88	77 145	1 795.12	77 145	20.52	77 145	12.02
kansas-3	87 424	3.25	87 976	2.26	87 976	61.39	87 976	10.76	87 976	36.08
kentucky-2	97 362	0.93	97 397	0.45	97 397	0.46	97 397	4.19	97 397	4.25
kentucky-3	97 906	3 077.14	100 510	1 292.90	99 918	3 684.53	100 507	35.39	100 511	160.03
louisiana-3	59 040	0.03	60 024	0.02	60 024	0.44	60 024	0.03	60 024	0.03
maine-3	26 231	< 0.01	26 734	< 0.01	26 734	< 0.01	26 734	< 0.01	26 734	< 0.01
maryland-3	44 539	0.07	45 496	0.04	45 496	0.54	45 496	0.03	45 496	0.03
massachusetts-2	139 799	0.02	140 095	0.05	140 095	0.10	140 095	0.03	140 095	0.03
massachusetts-3	144 381	2.22	145 866	0.41	145 866	1 292.74	145 866	11.06	145 866	11.58
mexico-2	94 820	< 0.01	94 834	< 0.01	94 834	0.01	94 834	< 0.01	94 834	< 0.01
mexico-3	96 700	0.07	97 663	0.02	97 663	8.94	97 663	0.10	97 663	0.10
minnesota-3	32 318	0.04	32 787	< 0.01	32 787	0.46	32 787	< 0.01	32 787	< 0.01
montana-3	59 521	0.18	59 822	0.10	59 822	3.37	59 753	0.02	59 753	0.02
nevada-3	51 269	0.01	52 036	< 0.01	52 036	0.19	52 036	< 0.01	52 036	< 0.01
new-hampshire-3	115 161	0.02	116 060	0.04	116 060	1.06	116 060	< 0.01	116 060	< 0.01
new-york-2	14 330	< 0.01	14 330	< 0.01	14 330	0.03	14 330	< 0.01	14 330	< 0.01
new-york-3	15 293	0.19	16 268	0.01	16 268	60.59	16 268	0.11	16 268	0.11
north-carolina-3	49 253	0.52	49 720	0.05	49 720	1 277.21	49 720	0.23	49 720	0.27
ohio-3	52 199	0.01	52 634	< 0.01	52 634	0.71	52 634	0.02	52 634	0.02
oregon-3	172 813	29.73	175 078	5.54	175 078	1 396.74	175 078	64.38	175 078	161.51
pennsylvania-3	142 472	0.02	143 870	0.02	143 870	1.33	143 870	< 0.01	143 870	0.01
puerto-rico-3	33 556	0.03	33 590	< 0.01	33 590	3.54	33 590	< 0.01	33 590	< 0.01
rhode-i.-2	179 366	0.46	184 596	0.14	184 596	0.86	184 596	0.60	184 596	0.18
rhode-i.-3	190 341	255.58	201 753	1 190.44	201 771	1 886.87	201 771	366.29	201 771	15.34

Continued on next page

Table 8 – Continued from previous page

Instance	HTWIS		HILS		M ² WIS + S		BASELINE		CHILS	
	ω	t	ω	t	ω	t	ω	t	ω	t
tennessee-3	32 232	< 0.01	32 276	< 0.01	32 276	0.07	32 276	< 0.01	32 276	< 0.01
utah-2	95 080	< 0.01	95 087	< 0.01	95 087	< 0.01	95 087	< 0.01	95 087	< 0.01
utah-3	97 754	0.05	98 847	0.06	98 847	1.34	98 847	0.10	98 847	0.10
vermont-2	57 563	0.04	59 310	1.91	59 310	1.07	59 284	< 0.01	59 310	42.52
vermont-3	60 518	4.89	63 304	667.25	63 312	1 317.01	63 302	4.38	63 302	4.41
virginia-2	290 535	0.03	295 867	0.13	295 867	0.11	295 867	0.12	295 867	0.12
virginia-3	300 335	1.38	308 305	1.34	308 305	1 297.87	308 305	3.63	308 305	3.61
washington-2	300 195	0.10	305 619	0.17	305 619	0.17	305 619	0.12	305 619	0.12
washington-3	305 019	14.41	314 288	546.60	314 288	1 373.62	314 288	115.04	314 288	161.81
west-virginia-3	46 344	0.32	47 927	0.31	47 927	62.72	47 927	0.74	47 927	0.74
snap as-skitter	124 141 373	1.17	123 207 288	3 597.32	124 157 729	2 828.19	124 141 585	3 545.45	124 111 689	3 491.32
com-amazon	19 270 078	0.18	19 266 084	3 590.70	19 271 031	0.45	19 270 569	3 571.05	19 270 939	3 556.41
loc-gowalla-edges	12 276 781	0.12	12 275 221	3 372.84	12 276 929	4.98	12 275 141	1 714.74	12 275 967	3 598.85
roadNet-CA	111 325 524	0.72	108 370 752	3 600.18	111 360 828	4.12	111 355 248	3 496.83	111 358 047	3 579.38
roadNet-PA	61 710 606	0.41	60 504 456	3 599.52	61 731 589	2.01	61 730 745	1 264.12	61 731 458	3 347.56
roadNet-TX	78 575 460	0.49	76 796 646	3 600.03	78 599 946	2.39	78 598 317	3 121.37	78 599 552	3 398.95
soc-LiveJ.	283 922 214	9.22	279 386 267	< 0.01	284 036 239	1 737.39	283 951 703	3 599.46	283 924 551	3 562.85
soc-p.-rel	83 920 370	39.06	82 984 397	3 598.22	81 112 447	3 637.19	83 971 405	3 369.22	83 982 856	3 520.91
web-BerkStan	43 889 843	14.87	43 694 574	3 599.51	43 907 482	4.29	43 895 988	2 790.96	43 901 482	3 600.08
web-Google	56 323 382	0.74	56 193 137	3 599.88	56 326 504	2.16	56 320 795	2 539.95	56 321 677	3 580.05
web-NotreDame	26 013 830	0.20	26 014 630	3 593.50	26 016 941	0.99	26 014 581	3 425.73	26 016 396	3 051.54
web-Stanford	17 789 430	0.57	17 779 603	3 595.78	17 792 930	1.31	17 792 392	2 784.70	17 792 474	3 491.05
ssmc ca2010	16 792 827	0.55	16 591 401	3 597.70	16 867 553	3 601.26	16 867 987	2 650.77	16 869 278	2 613.13
fl2010	8 719 272	0.40	8 694 303	3 599.61	8 743 506	183.77	8 742 384	2 941.69	8 743 309	2 832.06
ga2010	4 639 891	0.21	4 640 168	3 595.16	4 644 417	61.28	4 644 398	579.13	4 644 417	650.90
il2010	5 963 974	0.39	5 965 735	3 599.95	5 998 539	17.93	5 998 017	2 516.42	5 998 520	3 314.47
nh2010	587 059	0.04	588 843	2 811.97	588 996	0.44	588 996	15.57	588 996	28.91
ri2010	457 108	0.03	458 983	191.53	459 275	0.49	459 270	5.23	459 275	51.36

■ **Table 9** Average solution weight ω and time t (in seconds) required to compute it for the *reduced* instances from set one. The **best** solutions among all algorithms are marked bold.

Instance	HTWIS		HILS		M ² WIS + s		BASELINE		CHILS		
	ω	t	ω	t	ω	t	ω	t	ω	t	
fe	body	1 680 066	0.60	1 680 182	0.61	1 680 182	60.63	1 680 182	0.69	1 680 182	0.68
	pwt	1 169 768	2.21	1 178 273	1 946.51	1 178 735	3 196.24	1 178 735	9.31	1 178 735	9.84
	rotor	2 599 908	5.41	2 653 478	2 764.03	2 617 855	3 606.23	2 664 500	347.16	2 666 222	3 251.99
osm	alabama-3	184 863	1.52	185 744	1.46	185 744	304.35	185 744	1.47	185 744	1.46
	california-3	48 244	0.23	49 365	0.21	49 365	37.22	49 365	0.24	49 365	0.23
	d.-of-c.-2	206 445	6.24	209 132	5.97	209 132	1 284.78	209 132	5.90	209 132	5.86
	d.-of-c.-3	217 052	395.81	227 586	734.53	227 622	3 450.79	227 205	350.73	227 656	450.50
	florida-3	235 834	0.57	237 333	0.53	237 333	14.07	237 333	0.71	237 333	0.69
	georgia-3	220 585	0.42	222 652	0.39	222 652	8.90	222 652	0.40	222 652	0.40
	greenland-3	13 532	41.89	14 012	416.04	14 012	1 406.56	14 012	28.34	14 012	28.25
	hawaii-3	135 846	1 659.20	140 963	1 068.11	141 076	4 427.01	140 976	1 023.18	141 095	1 785.05
	idaho-3	76 227	59.61	77 145	52.11	77 145	1 499.48	77 145	185.03	77 145	200.46
	kansas-3	87 725	4.51	87 976	4.05	87 976	64.44	87 976	5.48	87 976	5.48
	kentucky-3	99 310	3 421.08	100 475	2 582.95	100 193	5 125.45	100 511	2 167.95	100 511	2 385.14
	massachusetts-3	144 574	4.01	145 866	3.09	145 866	1 293.42	145 866	3.57	145 866	3.57
	mexico-3	96 866	0.31	97 663	0.29	97 663	10.77	97 663	0.31	97 663	0.31
	montana-3	59 679	0.32	59 822	0.25	59 822	8.95	59 822	0.30	59 822	0.30
	new-york-3	15 666	0.49	16 268	0.46	16 268	62.24	16 268	0.44	16 268	0.44
	north-carolina-3	48 897	1.08	49 720	51.58	49 720	1 285.56	49 720	1.45	49 720	1.42
	oregon-3	173 454	35.28	175 078	24.02	175 078	1 410.40	175 078	25.52	175 078	25.46
	rhode-i.-2	184 554	0.57	184 596	0.52	184 596	5.79	184 596	0.55	184 596	0.55
	rhode-i.-3	197 126	306.81	201 654	184.23	201 767	3 171.02	201 480	167.51	201 771	333.07
	vermont-3	61 795	7.01	63 312	5.58	63 312	1 317.28	63 312	7.44	63 312	7.42
virginia-3	306 026	3.05	308 305	3.93	308 305	1 294.69	308 305	5.13	308 305	5.11	
washington-3	307 176	22.98	314 288	127.80	314 288	1 406.80	314 288	27.60	314 288	130.21	
west-virginia-3	47 074	0.70	47 927	0.69	47 927	68.22	47 927	0.59	47 927	0.59	
snap	as-skitter	124 156 703	3.46	124 157 729	8.63	124 157 729	1 300.24	124 157 700	3.45	124 157 729	33.49
	loc-gowalla-edges	12 276 850	0.33	12 276 929	0.33	12 276 929	3.76	12 276 929	0.34	12 276 929	0.34
	soc-LiveJ.	284 035 711	23.49	284 036 239	23.65	284 036 239	1 291.80	284 036 239	23.55	284 036 239	23.55
	soc-p.-rel	83 913 297	669.24	83 762 908	4 243.55	81 480 804	4 311.48	83 986 271	4 175.34	83 991 718	3 975.30
	web-NotreDame	26 016 941	0.62	26 016 941	0.62	26 016 941	0.73	26 016 941	0.62	26 016 941	0.62
ssmc	fl2010	8 742 642	3.62	8 743 506	37.95	8 743 506	1 479.03	8 743 506	3.65	8 743 506	3.65

■ **Table 10** Detailed graph properties for the first set consisting of *fe*, *mesh*, *osm*, *snap* and *ssmc* instances. Graphs marked with a \star are part of the parameter tuning set. We also present the number of vertices n_K and edges m_K of the instances reduced by LEARNANDREDUCE with the configuration *Fast - initial tight* as well as the computed offset and running time t_{red} in seconds.

	Instance	n	m	n_K	m_K	offset	t_{red}
fe	<i>body</i>	45 087	163 734	395	3 551	1 672 469	0.60
	<i>ocean</i>	143 437	409 593	0	0	7 248 581	3.56
	<i>pwt</i> \star	36 519	144 794	15 239	106 943	813 076	2.17
	<i>rotor</i> \star	99 617	662 431	89 294	690 242	435 335	5.05
	<i>sphere</i>	16 386	49 152	0	0	617 816	0.52
mesh	<i>blob</i>	16 068	24 102	0	0	855 547	0.03
	<i>buddha</i>	1 087 716	1 631 574	0	0	57 555 880	2.55
	<i>bunny</i>	68 790	103 017	0	0	3 686 960	0.13
	<i>dragonsub</i>	600 000	900 000	0	0	32 213 898	1.38
	<i>dragon</i>	150 000	225 000	0	0	7 956 530	0.20
	<i>ecat</i>	684 496	1 026 744	0	0	36 650 298	2.12
	<i>fandisk</i>	8 634	12 818	0	0	463 288	0.02
	<i>feline</i>	41 262	61 893	0	0	2 207 219	0.10
	<i>gameguy</i>	42 623	63 850	0	0	2 325 878	0.07
	<i>gargoyle</i>	20 000	30 000	0	0	1 059 559	0.04
	<i>turtle</i>	267 534	401 178	0	0	14 263 005	0.42
	osm	<i>alabama-2</i>	1 164	19 386	0	0	174 309
<i>alabama-3</i>		3 504	309 664	815	61 637	173 907	1.45
<i>california-2</i>		231	3 074	0	0	47 153	0.02
<i>california-3</i>		587	27 536	359	19 705	35 724	0.21
<i>canada-3</i>		943	20 241	0	0	86 018	0.23
<i>colorado-3</i>		538	8 365	0	0	54 741	0.01
<i>d.-of-c.-1</i>		2 500	24 651	0	0	196 475	0.22
<i>d.-of-c.-2</i>		13 597	1 609 795	2 361	274 529	178 323	5.76
<i>d.-of-c.-3</i>		46 221	27 729 137	26 728	13 406 329	133 708	290.37
<i>florida-3</i>		2 985	154 043	658	41 043	226 379	0.52
<i>georgia-3</i>		1 680	74 126	481	31 388	207 992	0.38
<i>greenland-2</i>		686	50 218	0	0	10 718	0.08
<i>greenland-3</i>		4 986	3 652 361	3 402	2 141 096	7 572	27.39
<i>hawaii-2</i>		2 875	265 158	0	0	125 284	0.15
<i>hawaii-3</i> \star		28 006	49 444 921	22 849	38 081 016	96 234	935.96
<i>idaho-3</i>		4 064	3 924 080	2 920	2 413 139	70 960	40.03
<i>kansas-3</i>		2 732	806 912	1 209	292 997	84 662	3.79
<i>kentucky-2</i>		2 453	643 428	0	0	97 397	0.27
<i>kentucky-3</i>		19 095	59 533 630	15 943	53 739 580	91 864	1 510.41
<i>louisiana-3</i>		1 162	37 077	0	0	60 024	0.08
<i>maine-3</i>		143	850	0	0	26 734	0.00
<i>maryland-3</i>		1 018	95 415	0	0	45 496	0.10
<i>massachusetts-2</i>		1 339	35 449	0	0	140 095	0.03
<i>massachusetts-3</i>	3 703	551 491	1 626	340 652	136 331	2.98	

Continued on next page

Table 10 – Continued from previous page

Instance	n	m	n_K	m_K	offset	t_{red}
<i>mexico-2</i>	516	9 411	0	0	94 834	0.01
<i>mexico-3</i>	1 096	47 131	447	20 443	86 467	0.29
<i>minnesota-3</i>	683	34 188	0	0	32 787	0.07
<i>montana-3</i>	837	69 293	382	39 859	55 531	0.25
<i>nevada-3</i>	569	15 016	0	0	52 036	0.02
<i>new-hampshire-3</i>	1 107	18 021	0	0	116 060	0.12
<i>new-york-2</i>	224	6 399	0	0	14 330	0.01
<i>new-york-3</i>	837	88 728	526	50 572	11 447	0.42
<i>north-carolina-3</i>	1 557	236 739	997	133 106	39 783	0.87
<i>ohio-3</i>	482	11 376	0	0	52 634	0.05
<i>oregon-3</i>	5 588	2 912 701	3 159	1 817 045	162 009	23.75
<i>pennsylvania-3</i>	1 148	26 464	0	0	143 870	0.12
<i>puerto-rico-3</i>	494	26 926	0	0	33 590	0.10
<i>rhode-i.-2</i>	2 866	295 488	498	46 183	174 013	0.52
<i>rhode-i.-3</i>	15 124	12 622 219	12 189	11 225 470	144 106	153.06
<i>tennessee-3</i>	212	3 215	0	0	32 276	0.01
<i>utah-2</i>	589	4 692	0	0	95 087	0.00
<i>utah-3</i>	1 339	42 872	0	0	98 847	0.28
<i>vermont-2</i>	766	37 607	0	0	59 310	0.11
<i>vermont-3*</i>	3 436	1 136 164	1 946	526 463	52 788	5.50
<i>virginia-2</i>	2 279	60 040	0	0	295 867	0.06
<i>virginia-3</i>	6 185	665 903	2 385	293 068	272 730	2.51
<i>washington-2</i>	3 025	152 449	0	0	305 619	0.10
<i>washington-3</i>	10 022	2 346 213	6 671	1 955 568	264 406	14.55
<i>west-virginia-3</i>	1 185	125 620	864	98 399	37 678	0.52
snap						
<i>as-skitter*</i>	1 696 415	11 095 298	1 951	27 277	124 100 687	3.43
<i>com-amazon</i>	334 863	925 869	0	0	19 271 031	0.32
<i>loc-gowalla-edges</i>	196 591	950 327	304	2 938	12 268 682	0.33
<i>roadNet-CA</i>	1 965 206	2 766 607	0	0	111 360 828	2.33
<i>roadNet-PA</i>	1 088 092	1 541 898	0	0	61 731 589	1.19
<i>roadNet-TX</i>	1 379 917	1 921 660	0	0	78 599 946	1.46
<i>soc-LiveJ.*</i>	4 847 571	42 851 237	1 715	28 390	283 975 051	23.47
<i>soc-p.-rel</i>	1 632 803	22 301 964	782 676	14 234 808	53 362 233	644.00
<i>web-BerkStan</i>	685 230	6 649 470	0	0	43 907 482	3.87
<i>web-Google</i>	875 713	4 322 051	0	0	56 326 504	2.03
<i>web-NotreDame</i>	325 729	1 090 108	97	1 357	26 013 618	0.62
<i>web-Stanford</i>	281 903	1 992 636	0	0	17 792 930	1.39
ssmc						
<i>ca2010</i>	710 145	1 744 683	0	0	16 869 550	7.34
<i>fl2010</i>	484 481	1 173 147	2 045	8 459	8 707 619	3.62
<i>ga2010</i>	291 086	709 028	0	0	4 644 417	0.89
<i>il2010</i>	451 554	1 082 232	0	0	5 998 539	5.63
<i>nh2010</i>	48 837	117 275	0	0	588 996	0.16
<i>ri2010</i>	25 181	62 875	0	0	459 275	0.19

■ **Table 11** Detailed graph properties for the second set of vehicle routing instances. We also present the number of vertices n_K and edges m_K of the instances reduced by LEARNANDREDUCE with the configuration *Fast - initial tight* as well as the computed offset and running time t_{red} in seconds.

Instance	n	m	n_K	m_K	offset	t_{red}
★ <i>CR-S-L-1</i>	863 368	331 203 970	855 833	328 396 194	26 070	3 671.65
<i>CR-S-L-2</i>	880 974	342 158 741	873 941	339 503 913	20 282	5 234.35
<i>CR-S-L-4</i>	881 910	344 057 350	874 668	341 151 292	19 400	5 315.89
<i>CR-S-L-6</i>	578 244	219 717 582	572 888	217 572 336	25 208	3 056.68
<i>CR-S-L-7</i>	270 067	94 109 215	266 591	92 817 339	26 955	858.97
<i>CR-T-C-1</i>	602 472	194 753 152	594 883	192 451 235	59 577	2 668.29
<i>CR-T-C-2</i>	652 497	215 694 927	645 058	213 228 808	32 598	2 870.86
<i>CR-T-D-4</i>	651 861	220 480 534	644 845	218 142 885	22 898	2 342.34
<i>CR-T-D-6</i>	381 380	115 082 762	376 351	113 599 041	31 498	1 393.38
<i>CR-T-D-7</i>	163 809	43 028 583	160 630	42 184 292	29 046	341.15
<i>CW-S-L-1</i>	411 950	283 860 106	409 559	282 656 866	11 718	4 465.88
<i>CW-S-L-2</i>	443 404	315 569 883	441 093	314 281 707	8 310	5 816.47
★ <i>CW-S-L-4</i>	430 379	303 042 962	427 984	301 676 399	6 009	5 262.94
<i>CW-S-L-6</i>	267 698	171 132 761	265 820	170 150 154	9 603	2 512.19
<i>CW-S-L-7</i>	127 871	78 459 291	126 866	77 941 263	4 283	859.79
<i>CW-T-C-1</i>	266 403	144 634 578	264 389	143 674 135	10 530	2 064.78
★ <i>CW-T-C-2</i>	194 413	111 098 006	192 871	110 337 336	10 128	1 387.53
<i>CW-T-D-4</i>	83 091	37 881 529	82 110	37 453 654	3 108	356.97
<i>CW-T-D-6</i>	83 758	38 781 839	82 723	38 299 758	5 338	400.99
<i>MR-D-03</i>	21 499	130 508	17 390	131 591	832 349 816	1.06
<i>MR-D-05</i>	27 621	236 044	24 250	236 758	676 962 870	1.86
★ <i>MR-D-FN</i>	30 467	296 369	27 301	297 905	639 582 861	2.46
<i>MR-W-FN</i>	15 639	126 800	14 657	128 925	691 250 460	0.75
<i>MT-D-01</i>	979	3 125	0	0	238 166 485	0.02
<i>MT-D-200</i>	10 880	505 359	10 676	493 364	6 914 835	2.19
<i>MT-D-FN</i>	10 880	604 041	10 682	595 799	45 784 382	2.33
<i>MT-W-01</i>	1 006	2 411	0	0	312 121 568	< 0.01
<i>MT-W-200</i>	12 320	515 871	11 472	474 079	85 332 696	2.33
<i>MT-W-FN</i>	12 320	553 895	11 456	503 617	128 611 366	2.43
<i>MW-D-01</i>	3 988	13 556	2 539	13 853	307 196 278	0.18
<i>MW-D-20</i>	20 054	606 318	19 473	600 915	104 526 987	3.15
★ <i>MW-D-40</i>	33 563	1 879 303	33 062	1 870 537	74 805 076	8.33
<i>MW-D-FN</i>	47 504	4 017 196	47 070	4 005 378	60 228 177	18.80
<i>MW-W-01</i>	3 079	22 664	2 844	22 765	169 735 181	0.16
★ <i>MW-W-05</i>	10 790	485 261	10 667	481 661	25 259 548	1.68
<i>MW-W-10</i>	18 023	1 451 813	17 921	1 445 959	16 146 685	4.81
<i>MW-W-FN</i>	22 316	2 275 623	22 215	2 269 047	15 670 946	9.86